Precision QCD in DIS at HERA

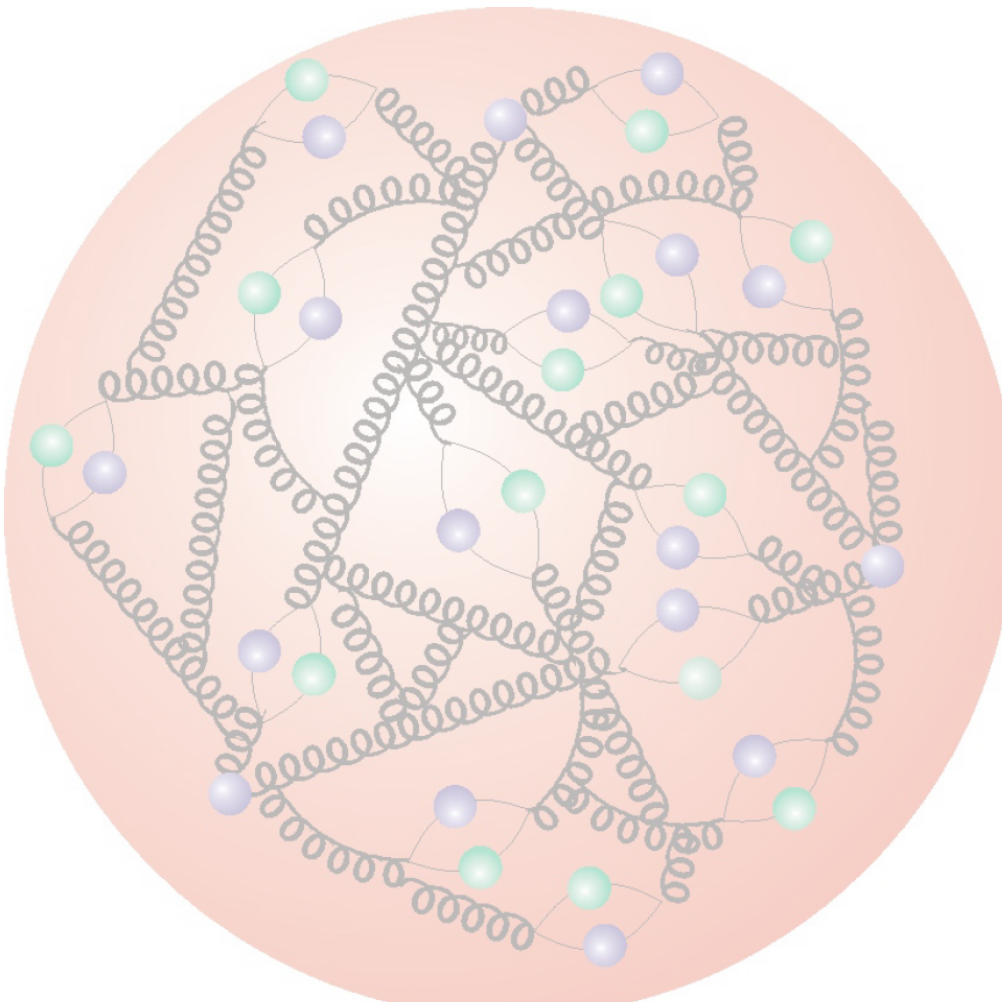

- Introduction
- HERA-II Updates
- H1 NC/CC $e^{\pm}p$
- H1 NC High y $e^{\pm}p$
- ZEUS NC $e^{+}p$
- HERAPDF Plans

Queen Mary
University of London

Eram Rizvi

PDF4LHC

IPPP, Durham – 26th Sept. 2012

H1

ZEUS

Where Are We Going?

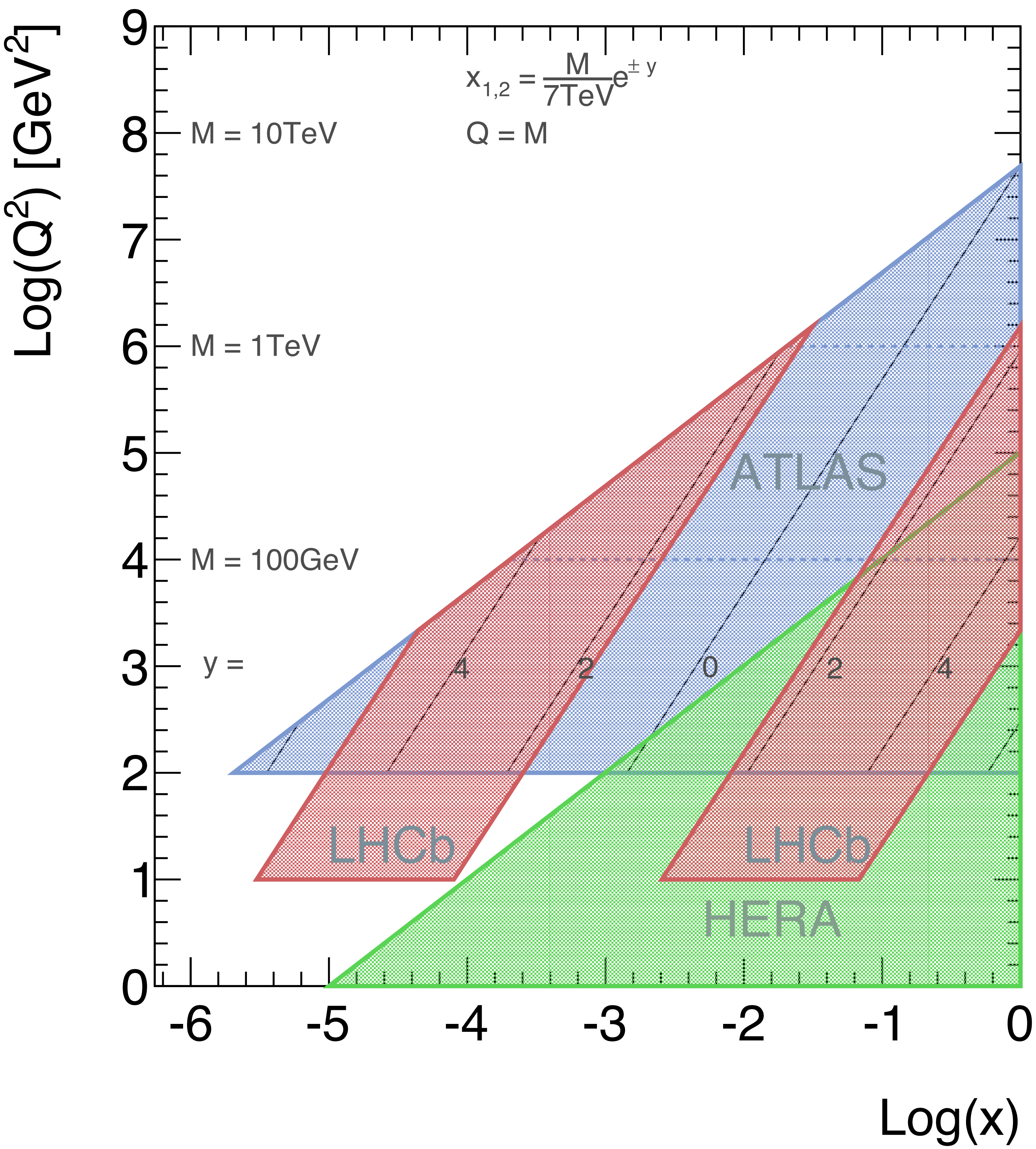

LHC: largest mass states at large x

For central production $x = x_1 = x_2$

$$M = x\sqrt{s}$$

i.e. M > 1 TeV probes x>0.1

Searches for high mass states require precision knowledge at high x

Z′ / quantum gravity / susy searches...

DGLAP evolution allows predictions to be made

High x predictions rely on

- data (DIS / fixed target)
- sum rules
- behaviour of PDFs as $x \rightarrow 1$

Structure Functions

$$\frac{d\sigma^{\pm}_{NC}}{dxdQ^2} = \frac{2\pi\alpha^2}{x}\left[\frac{1}{Q^2}\right]^2\left[Y_+\tilde{F}_2 \mp Y_- x\tilde{F}_3 - y^2\tilde{F}_L\right]$$

$$\frac{d\sigma^{\pm}_{CC}}{dxdQ^2} = \frac{G_F^2}{4\pi x}\left[\frac{M_W^2}{M_W^2+Q^2}\right]^2\left[Y_+\tilde{W}_2^{\pm} \mp Y_- x\tilde{W}_3^{\pm} - y^2\tilde{W}_L^{\pm}\right]$$

$$Y_{\pm} = 1 \pm (1-y)^2$$

$\tilde{F}_2 \propto \sum(xq_i + x\bar{q}_i)$ Dominant contribution

$x\tilde{F}_3 \propto \sum(xq_i - x\bar{q}_i)$ Only sensitive at high $Q^2 \sim M_Z^2$

$\tilde{F}_L \propto \alpha_s \cdot xg(x,Q^2)$ Only sensitive at low Q^2 and high y

similarly for pure weak CC analogues:

$W_2^{\pm}$, $xW_3^{\pm}$ and $W_L^{\pm}$

The NC reduced cross section defined as:

$$\tilde{\sigma}^{\pm}_{NC} = \frac{Q^2 x}{2\alpha\pi^2}\frac{1}{Y_+}\frac{d^2\sigma^{\pm}}{dxdQ^2}$$

$$\tilde{\sigma}^{\pm}_{NC} \sim \tilde{F}_2 \mp \frac{Y_-}{Y_+}x\tilde{F}_3$$

The CC reduced cross section defined as:

$$\sigma^{\pm}_{CC} = \frac{2\pi x}{G_F^2}\left[\frac{M_W^2+Q^2}{M_W^2}\right]^2\frac{d\sigma^{\pm}_{CC}}{dxdQ^2}$$

$$\frac{d\sigma^{\pm}_{CC}}{dxdQ^2} = \frac{1}{2}\left[Y_+ W_2^{\pm} \mp Y_- xW_3^{\pm} - y^2 W_L^{\pm}\right]$$

H1 and ZEUS

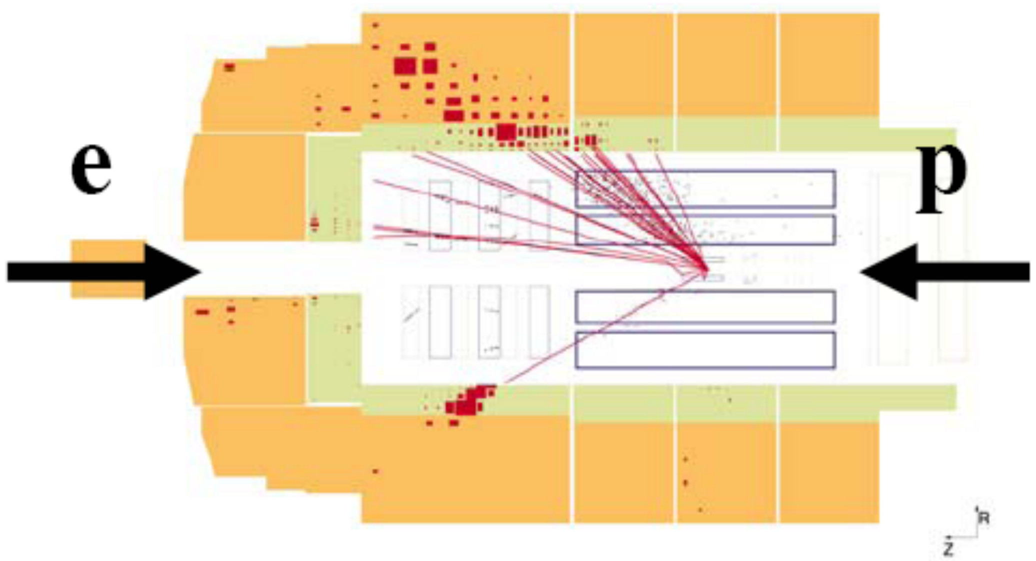

Neutral current event selection:

High P_T isolated scattered lepton
Suppress huge photo-production background by imposing longitudinal energy-momentum conservation

Kinematics may be reconstructed in many ways:
energy/angle of hadrons & scattered lepton
provides excellent tools for sys cross checks

Removal of scattered lepton provides a
high stats "pseudo-charged current sample"
Excellent tool to cross check CC analysis

Final selection: ~10^5 events per sample at high Q^2
~10^7 events for $10 < Q^2 < 100$ GeV^2

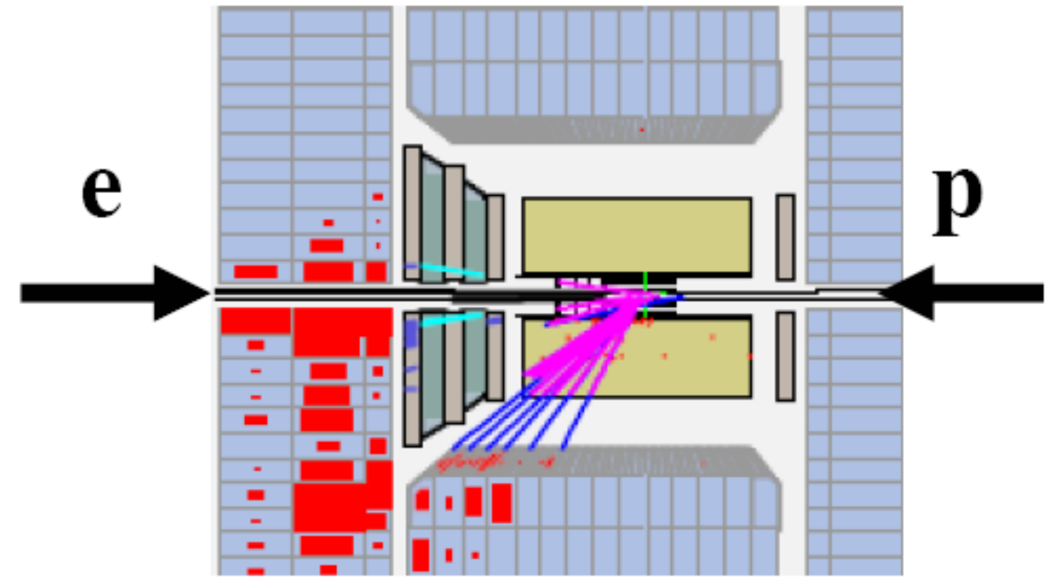

Charged current event selection:

Large missing transverse momentum (neutrino)

Suppress huge photo-production background

Topological finders to remove cosmic muons

Kinematics reconstructed from hadrons

Final selection: ~10^3 events per sample

<u>HERA-I operation 1993-2000</u>
Ee = 27.6 GeV
Ep = 820 / 920 GeV
$\int\mathcal{L} \sim 110\ pb^{-1}$ per experiment

<u>HERA-II operation 2003-2007</u>
Ee = 27.6 GeV
Ep = 920 GeV
$\int\mathcal{L} \sim 330\ pb^{-1}$ per experiment
Longitudinally polarised leptons

<u>Low Energy Run 2007</u>
Ee = 27.6 GeV
Ep = 575 & 460 GeV
Dedicated F_L measurement

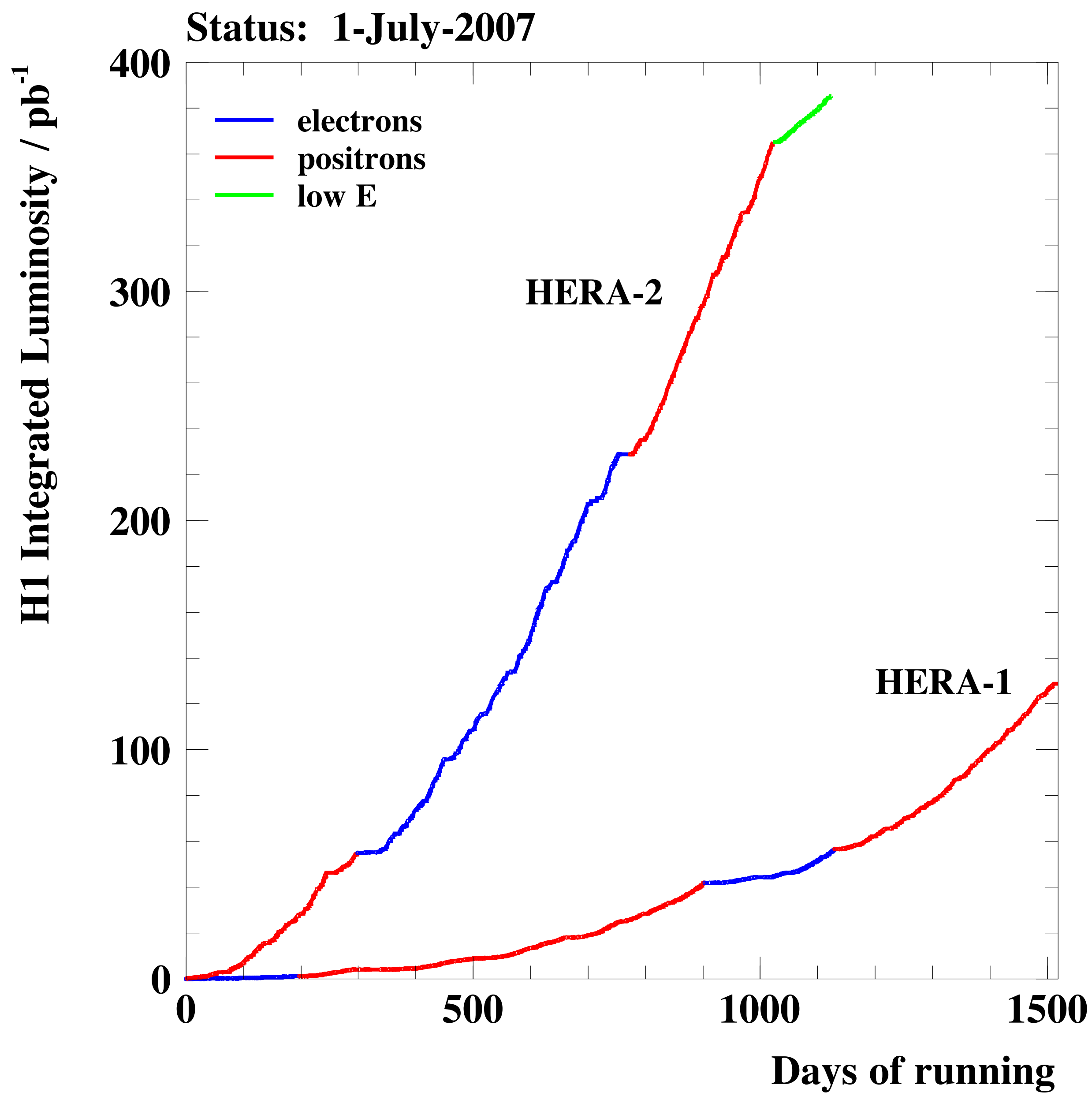

HERA Structure Function Data

Summary of HERA-I datasets
Combined in HERAPDF1.0

Available since 2009

Data Set		x Range		Q^2 Range GeV^2		$\mathcal{L}$ pb^{-1}	e^+/e^-	$\sqrt{s}$ GeV
H1 svx-mb	95-00	5×10^{-6}	0.02	0.2	12	2.1	e^+p	301-319
H1 low Q^2	96-00	2×10^{-4}	0.1	12	150	22	e^+p	301-319
H1 NC	94-97	0.0032	0.65	150	30000	35.6	e^+p	301
H1 CC	94-97	0.013	0.40	300	15000	35.6	e^+p	301
H1 NC	98-99	0.0032	0.65	150	30000	16.4	e^-p	319
H1 CC	98-99	0.013	0.40	300	15000	16.4	e^-p	319
H1 NC HY	98-99	0.0013	0.01	100	800	16.4	e^-p	319
H1 NC	99-00	0.0013	0.65	100	30000	65.2	e^+p	319
H1 CC	99-00	0.013	0.40	300	15000	65.2	e^+p	319
ZEUS BPC	95	2×10^{-6}	6×10^{-5}	0.11	0.65	1.65	e^+p	301
ZEUS BPT	97	6×10^{-7}	0.001	0.045	0.65	3.9	e^+p	301
ZEUS SVX	95	1.2×10^{-5}	0.0019	0.6	17	0.2	e^+p	301
ZEUS NC	96-97	6×10^{-5}	0.65	2.7	30000	30.0	e^+p	301
ZEUS CC	94-97	0.015	0.42	280	17000	47.7	e^+p	301
ZEUS NC	98-99	0.005	0.65	200	30000	15.9	e^-p	319
ZEUS CC	98-99	0.015	0.42	280	30000	16.4	e^-p	319
ZEUS NC	99-00	0.005	0.65	200	30000	63.2	e^+p	319
ZEUS CC	99-00	0.008	0.42	280	17000	60.9	e^+p	319

High Q^2 NC and CC data limited to
100 pb^{-1} e^+p
16 pb^{-1} e^-p

HERA Structure Function Data

Up till now HERA-II datasets only partially published

ZEUS CC e^-p	175 pb^{-1}	EPJ C 61 (2009) 223-235
ZEUS CC e^+p	132 pb^{-1}	EPJ C 70 (2010) 945-963
ZEUS NC e^-p	170 pb^{-1}	EPJ C 62 (2009) 625-658
ZEUS NC e^+p	135 pb^{-1}	ZEUS-prel-11-003
H1 CC e^-p	149 pb^{-1}	H1prelim-09-043
H1 CC e^+p	180 pb^{-1}	H1prelim-09-043
H1 NC e^-p	149 pb^{-1}	H1prelim-09-042
H1 NC e^+p	180 pb^{-1}	H1prelim-09-042

HERA-II datasets
Combined in HERAPDF1.5
(except ZEUS NC e^+p)

breakdown of HERA-II data samples

	R	L
e^-p	$\mathcal{L} = 47.3\,\mathrm{pb}^{-1}$ $P_e = (+36.0 \pm 1.0)\%$	$\mathcal{L} = 104.4\,\mathrm{pb}^{-1}$ $P_e = (-25.8 \pm 0.7)\%$
e^+p	$\mathcal{L} = 101.3\,\mathrm{pb}^{-1}$ $P_e = (+32.5 \pm 0.7)\%$	$\mathcal{L} = 80.7\,\mathrm{pb}^{-1}$ $P_e = (-37.0 \pm 0.7)\%$

ZEUS CC e^-p	175 pb^{-1}	EPJ C 61 (2009) 223-235
ZEUS CC e^+p	132 pb^{-1}	EPJ C 70 (2010) 945-963
ZEUS NC e^-p	170 pb^{-1}	EPJ C 62 (2009) 625-658
ZEUS NC e^+p	135 pb^{-1}	**arXiv:1208.6138**
H1 CC e^-p	149 pb^{-1}	**arXiv:1206.7007**
H1 CC e^+p	180 pb^{-1}	
H1 NC e^-p	149 pb^{-1}	
H1 NC e^+p	180 pb^{-1}	

Complete the analyses of HERA high Q^2 inclusive structure function data

New published data increase $\int\mathcal{L}$ by
~ factor 3 for e^+p
~ factor 10 for e^-p
much improved systematic uncertainties

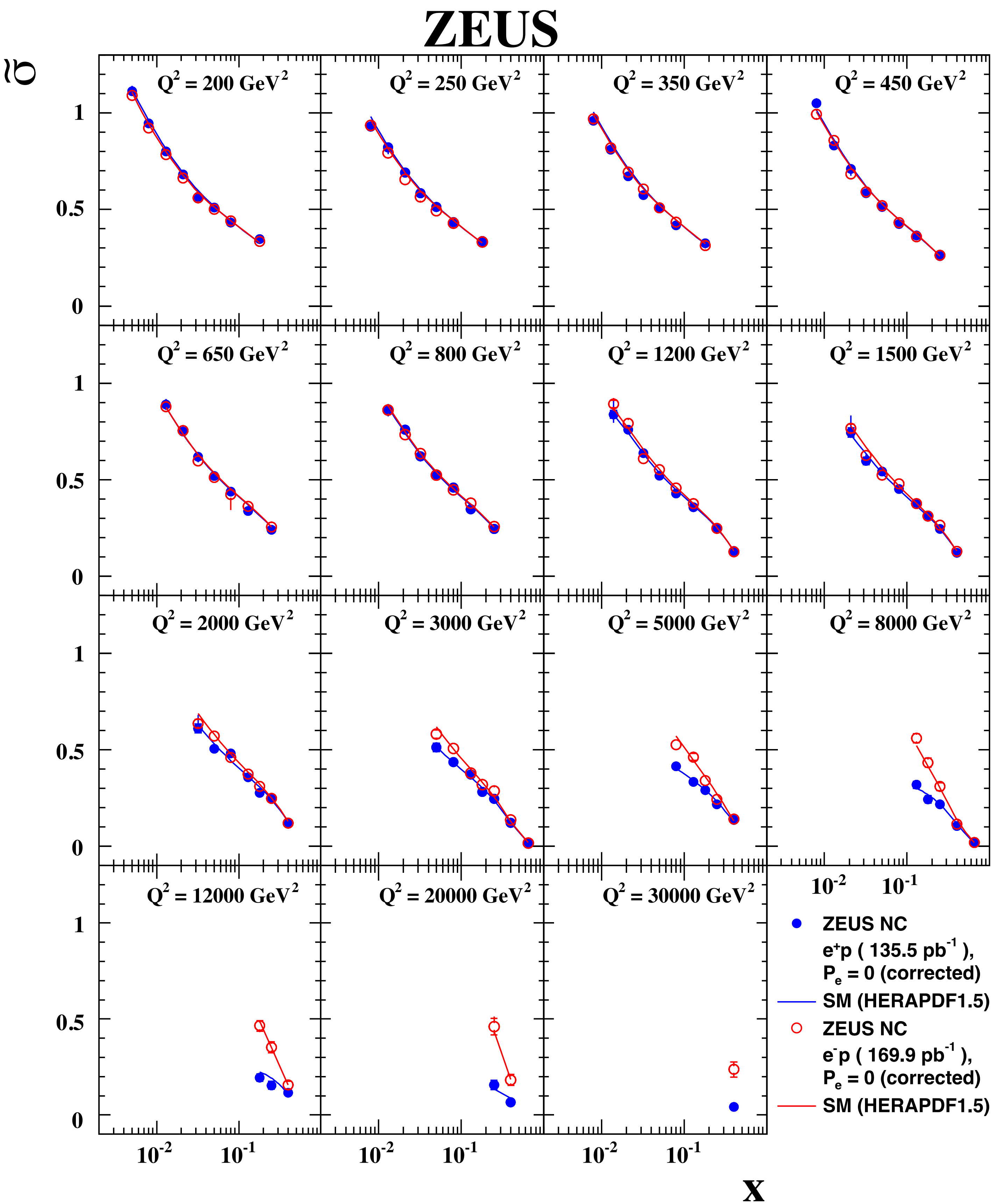

High Q^2 is the EW physics regime

Final measurement of ZEUS NC e^+p data

Shown here for P=0
Polarised measurements also available

Compared to published NC e^-p data

High Q^2 NC Cross Sections

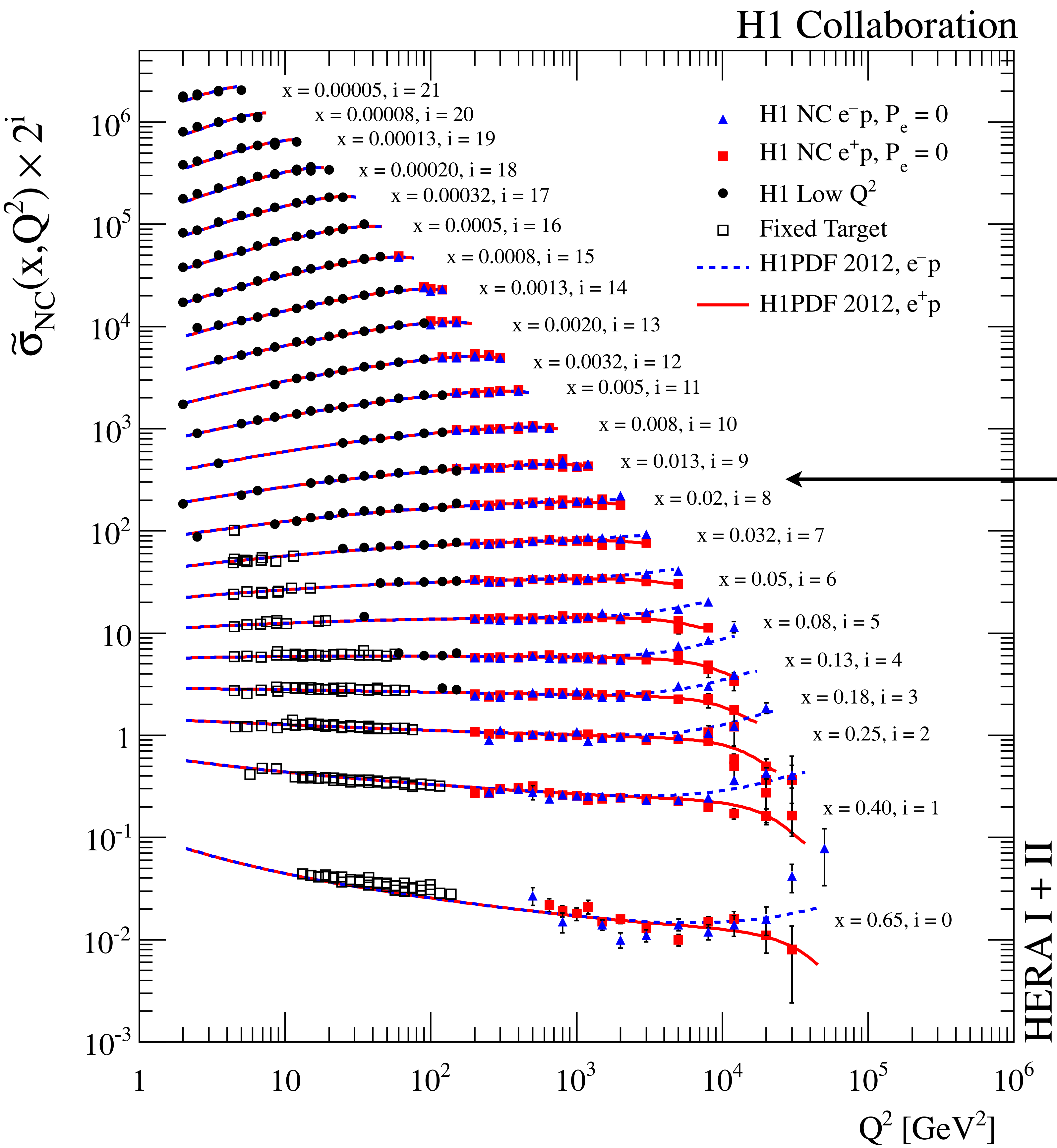

H1 precision 1.5% for $Q^2 < 500$ GeV^2

⇒ factor 2 reduction in error wrt HERA-I

Statistics limited at higher Q^2 and high x

Extended reach at high x compared to H1 preliminary data

This x region is the 'sweet spot'
High precision with long Q^2 lever arm
x-range relevant for Higgs production

Combination of high Q^2 data HERA-I and HERA-II

Larger HERA-II luminosity

→ improved precision at high x / Q^2

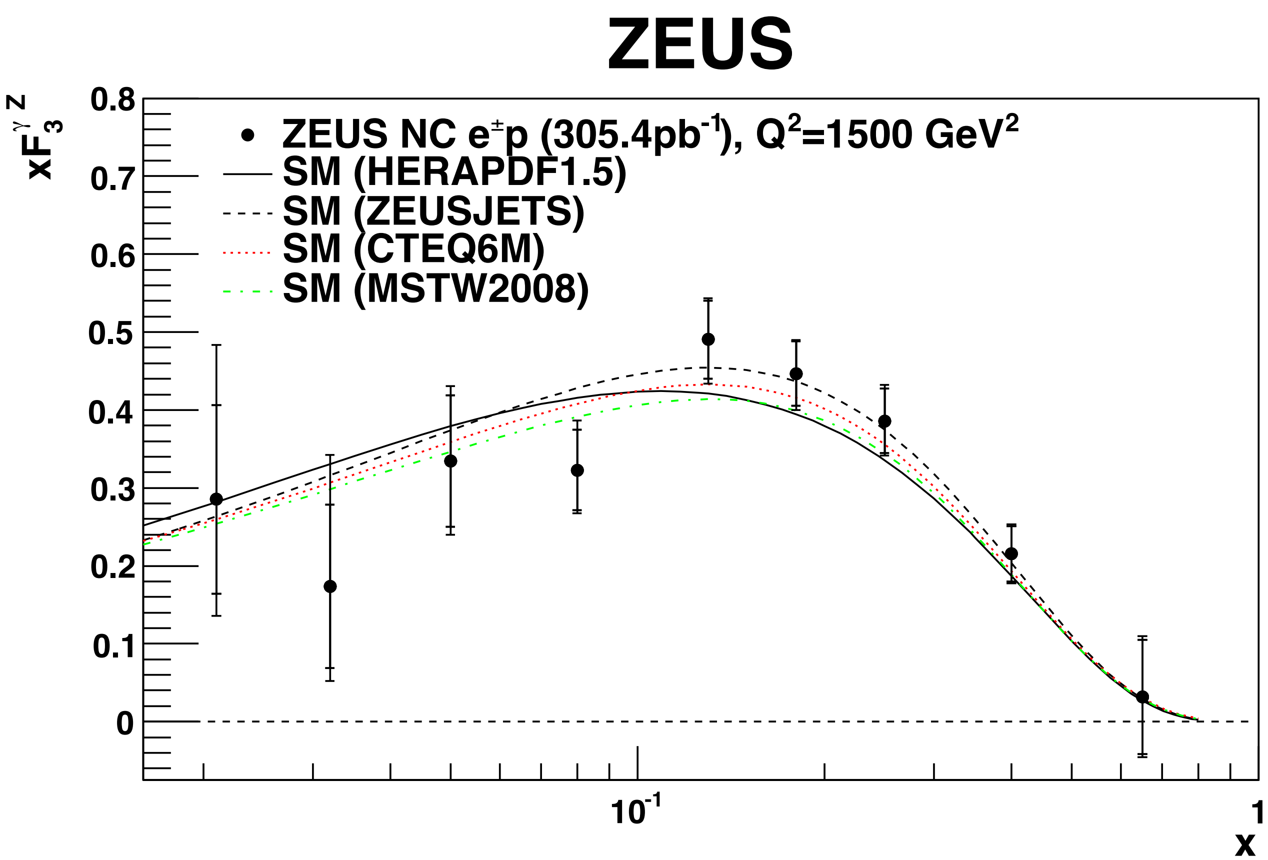

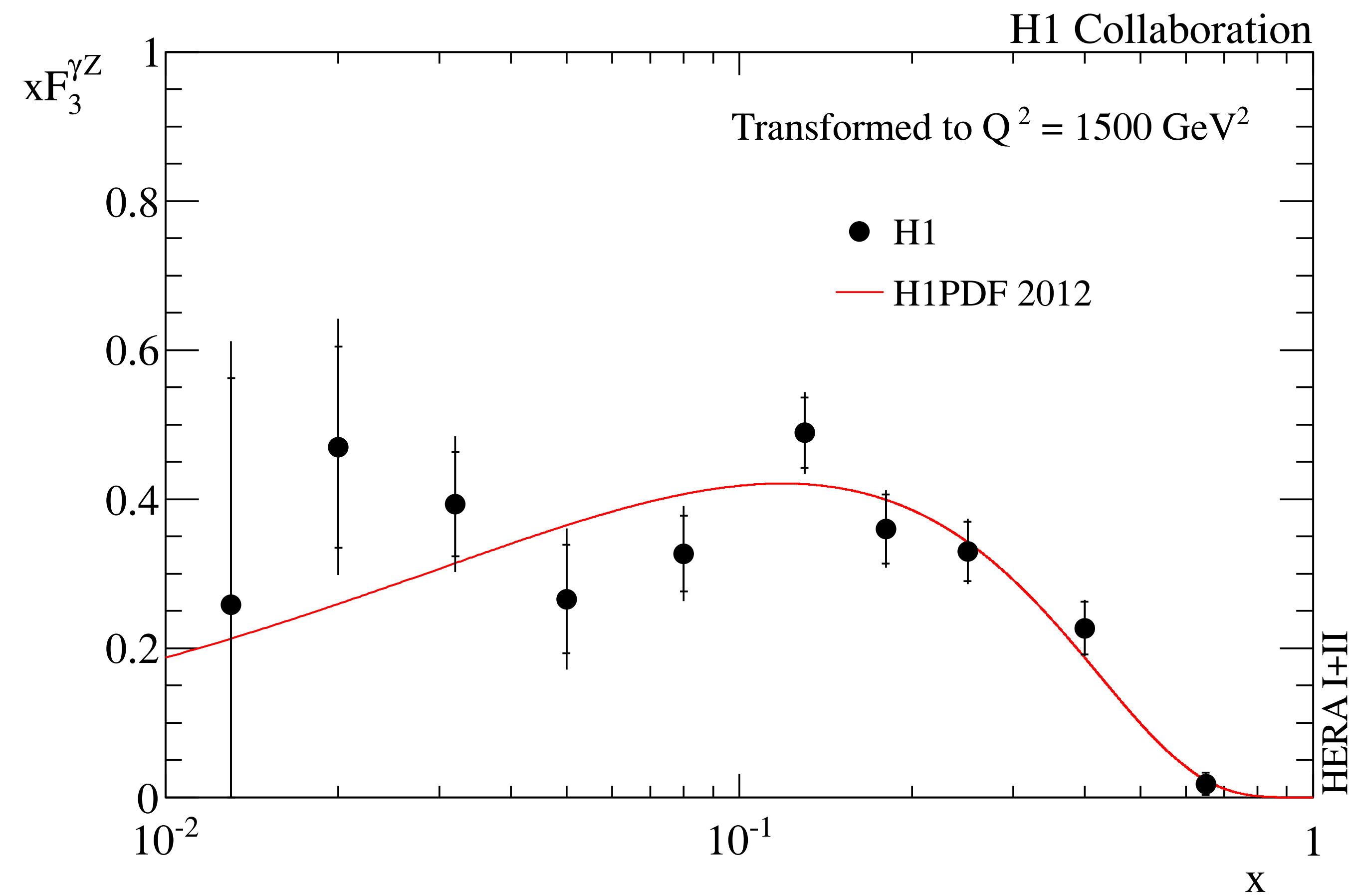

At high Q^2 xF_3 arises due to Z^0 effects
enhanced e^- cross section wrt e^+
Difference is xF_3
Sensitive to valence PDFs

$$x\tilde{F}_3 = \frac{Y_+}{2Y_-}(\tilde{\sigma}^-_{NC} - \tilde{\sigma}^+_{NC}) \approx a_e \chi_Z x F_3^{\gamma Z}$$

$$x\tilde{F}_3 \propto \sum (xq_i - x\bar{q}_i)$$

H1 measure integral of $xF_3^{\gamma Z}$ - validate sumrule:

$$\int_{0.016}^{0.725} \mathrm{d}x\ F_3^{\gamma Z}(x, Q^2 = 1\,500\,\mathrm{GeV}^2) = 1.22 \pm 0.09(\mathrm{stat}) \pm 0.07(\mathrm{syst})$$

LO integral predicted to be $5/3 + \mathcal{O}(\alpha_S/\pi)$

NC Cross Sections at High y

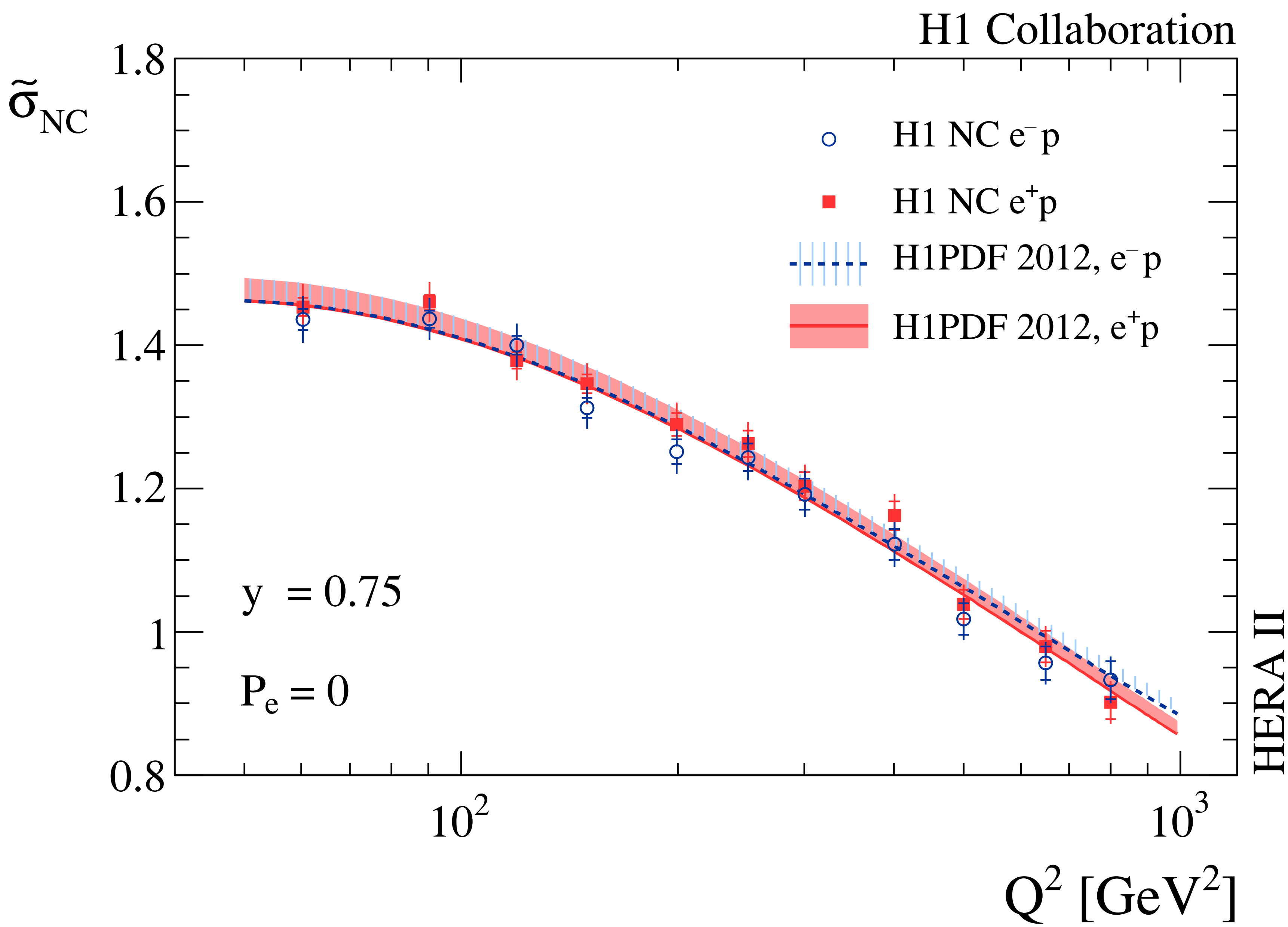

Measurement extension to high y at high Q^2

Sensitive to F_L and xg

Difficult measurement:
- low scattered electron energy $E_e' > 5$ GeV
- large photoproduction background

Total uncertainty reduced by factor 2:
HERA-I ~4%
HERA-II ~2%

Electron scattering

Positron scattering

$$\frac{d^2\sigma^-_{CC}}{dxdQ^2} = \frac{G_F^2}{2\pi}\left(\frac{M_W^2}{M_W^2+Q^2}\right)^2\left[(u+c)+(1-y)^2(\bar{d}+\bar{s})\right]$$

$$\frac{d^2\sigma^+_{CC}}{dxdQ^2} = \frac{G_F^2}{2\pi}\left(\frac{M_W^2}{M_W^2+Q^2}\right)^2\left[(\bar{u}+\bar{c})+(1-y)^2(d+s)\right]$$

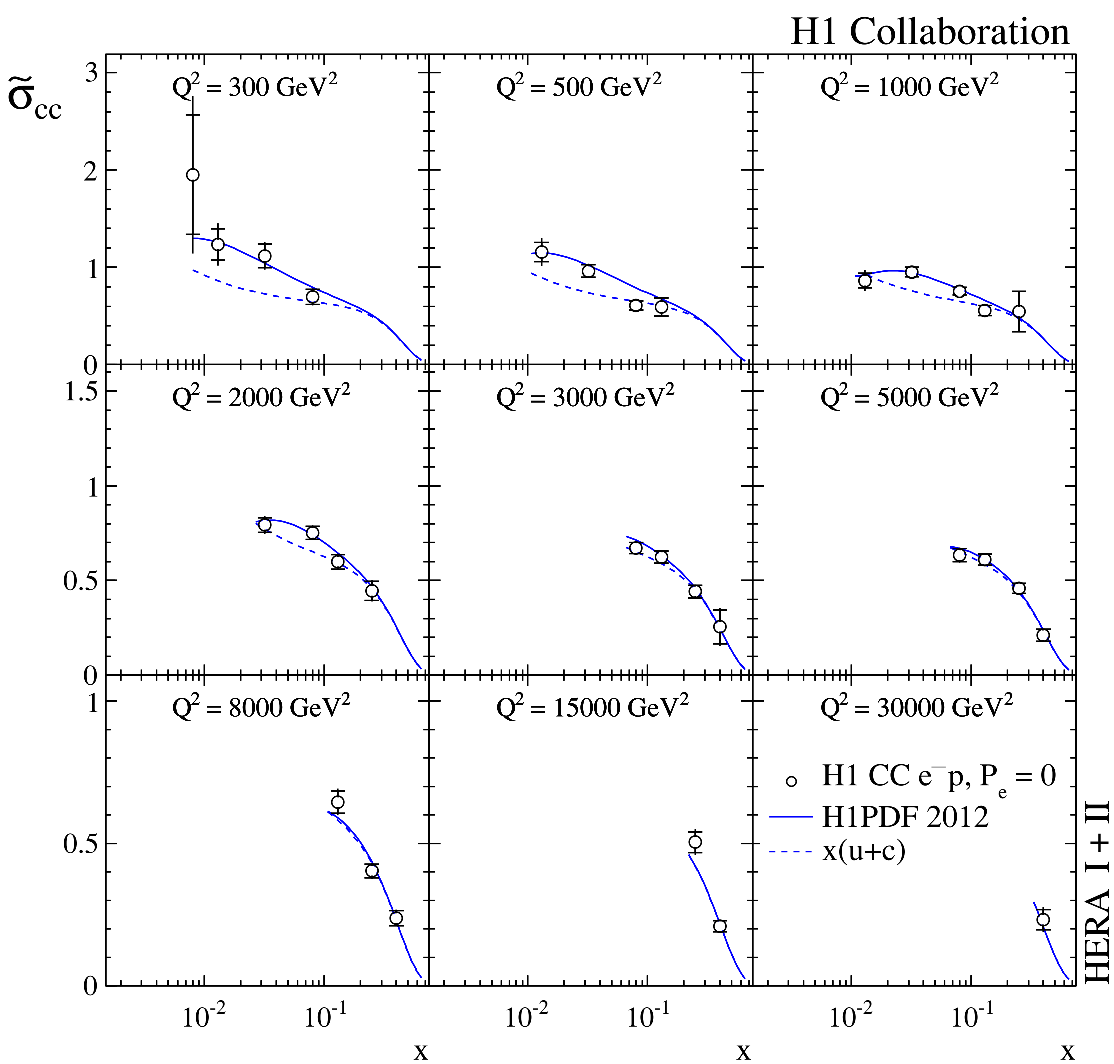

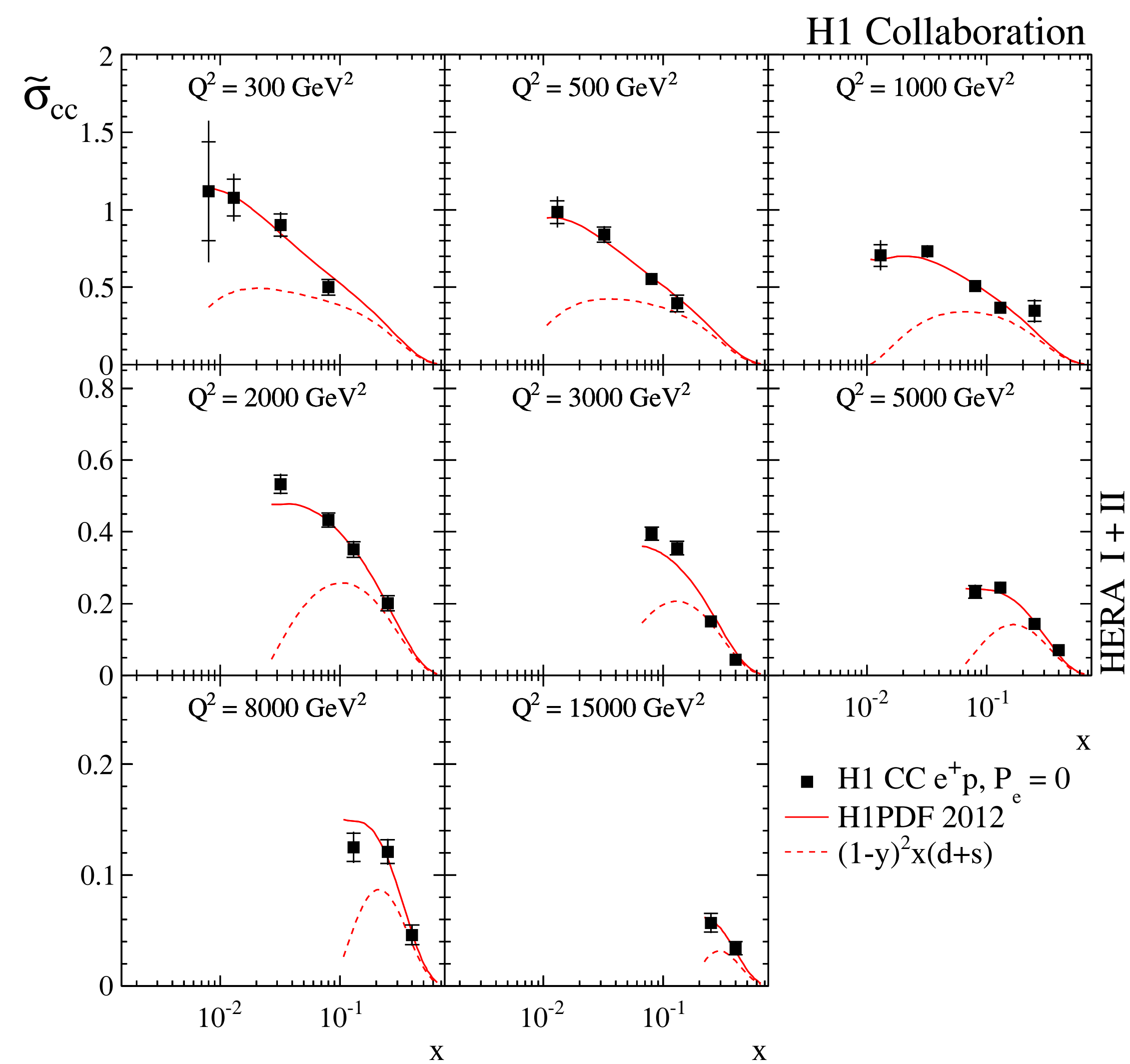

H1 combination of high Q^2 CC data (HERA-I+II)
Improvement of total uncertainty
Dominated by statistical errors
Provide important flavour decomposition information

CC e+ data provide strong d_v constraint at high x
Precision limited by statistics: typically 5-10%
HERA-I precision of 10-15% for e+p
Large gain to come after combination with ZEUS

CC Polarisation Dependence

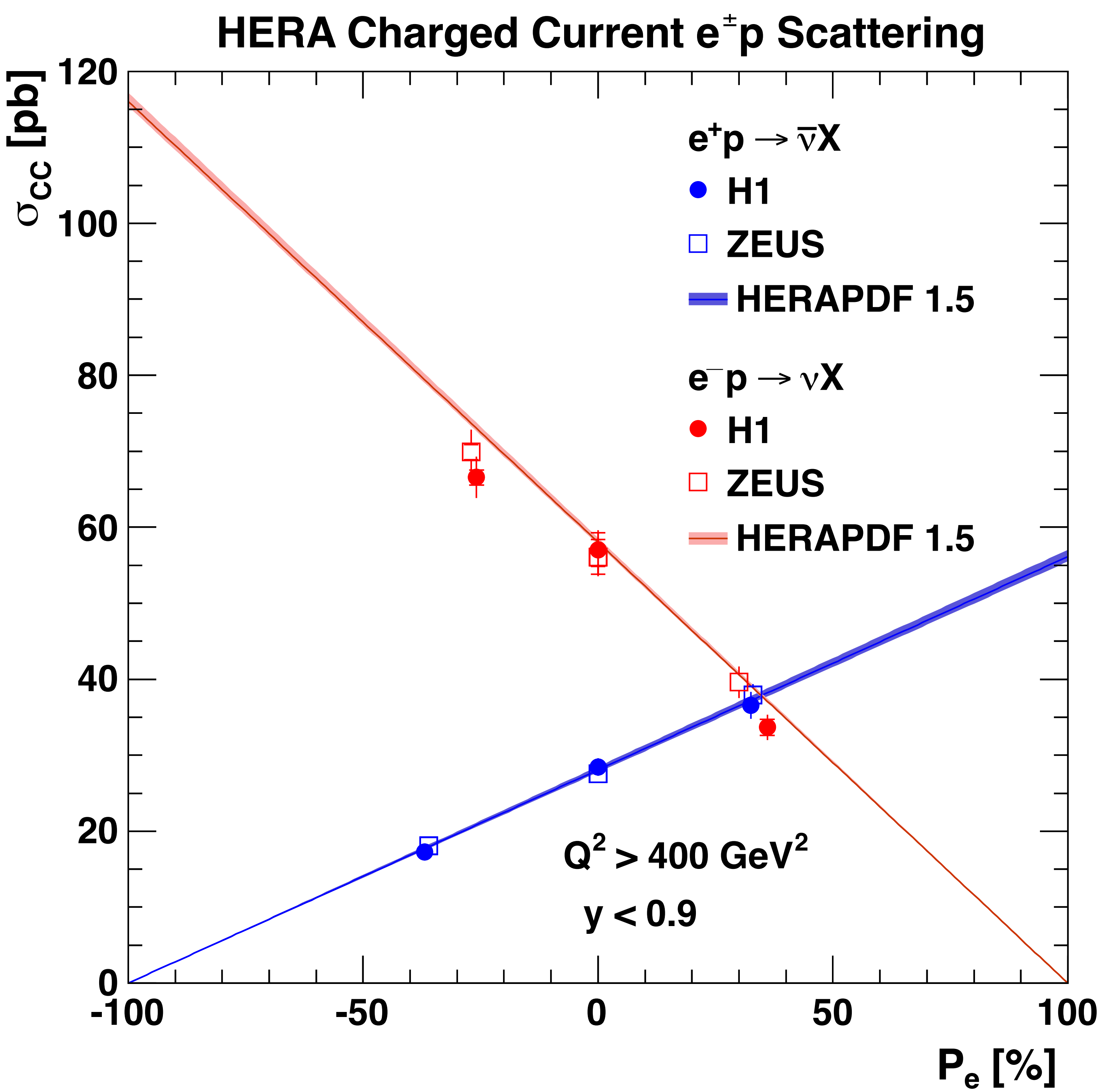

Polarisation dependence of CC cross section now final from H1 and ZEUS

Polarised NC Cross Sections

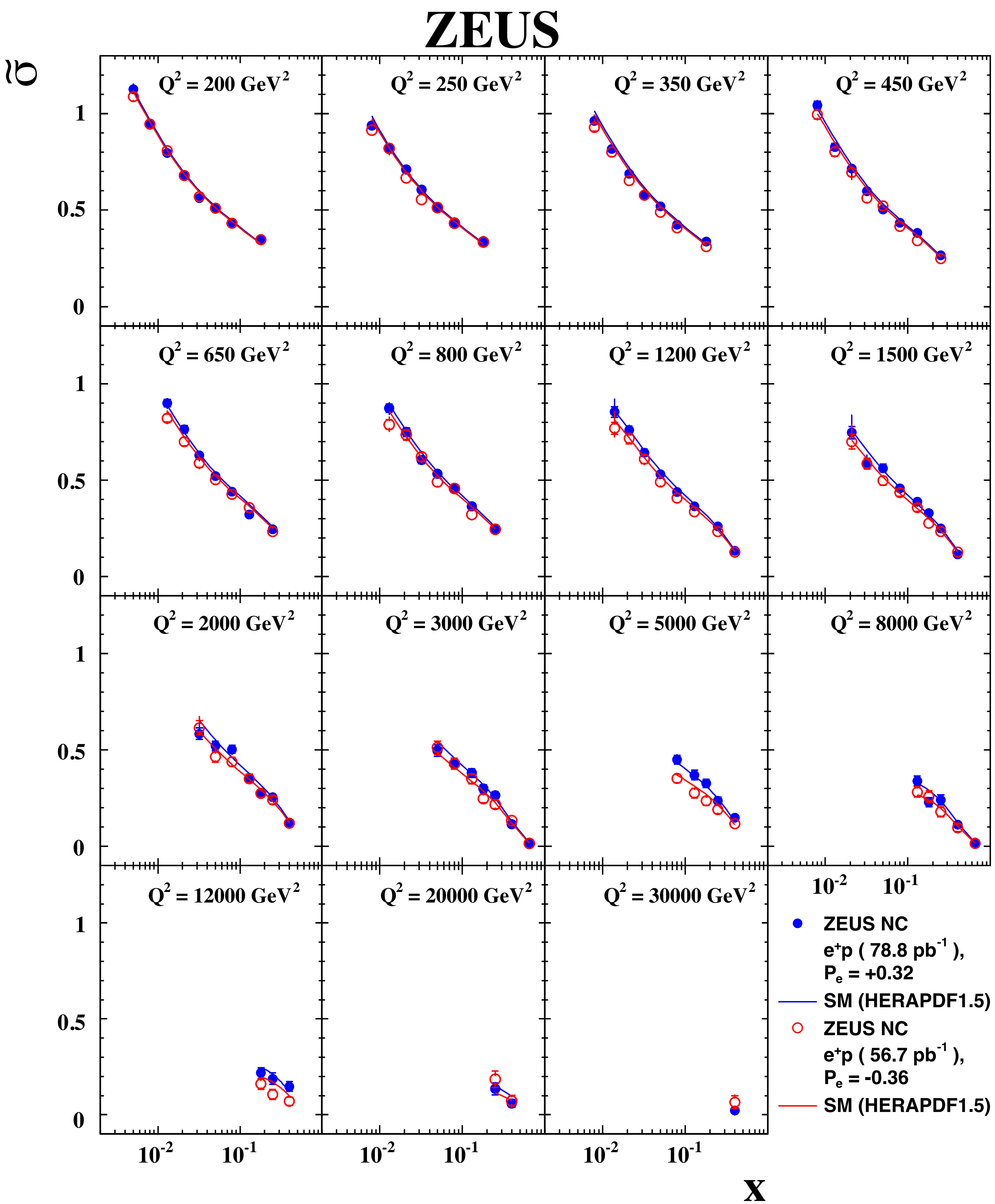

Polarised NC measurements completed for e^+p , e^-p , L-handed , R-handed scattering

Difference in L,R scattering visible at high Q^2

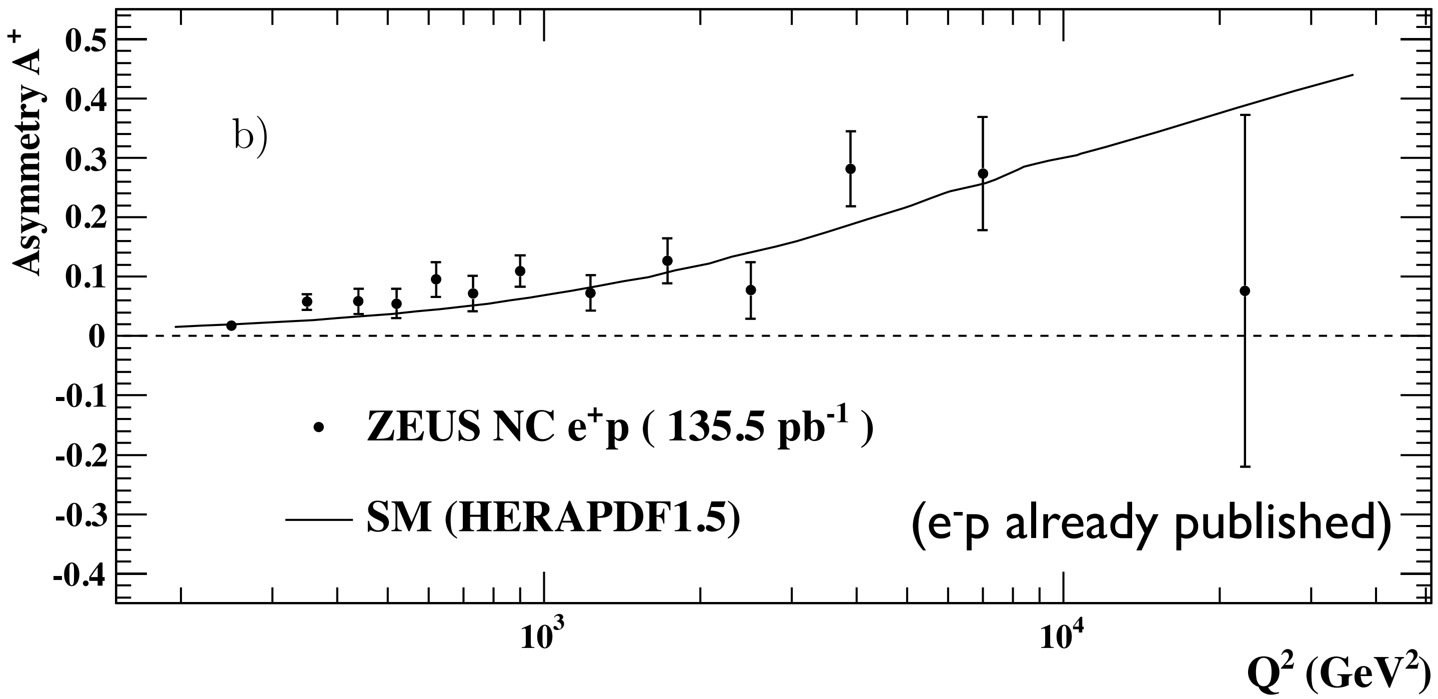

NC polarisation asymmetry:

$$A^{\pm} = \frac{2}{P_L^{\pm} - P_R^{\pm}} \cdot \frac{\sigma^{\pm}(P_L^{\pm}) - \sigma^{\pm}(P_R^{\pm})}{\sigma^{\pm}(P_L^{\pm}) + \sigma^{\pm}(P_R^{\pm})}$$

At large x $A^{\pm} \propto \pm\kappa \frac{1 + d_v/u_v}{4 + d_v/u_v}$

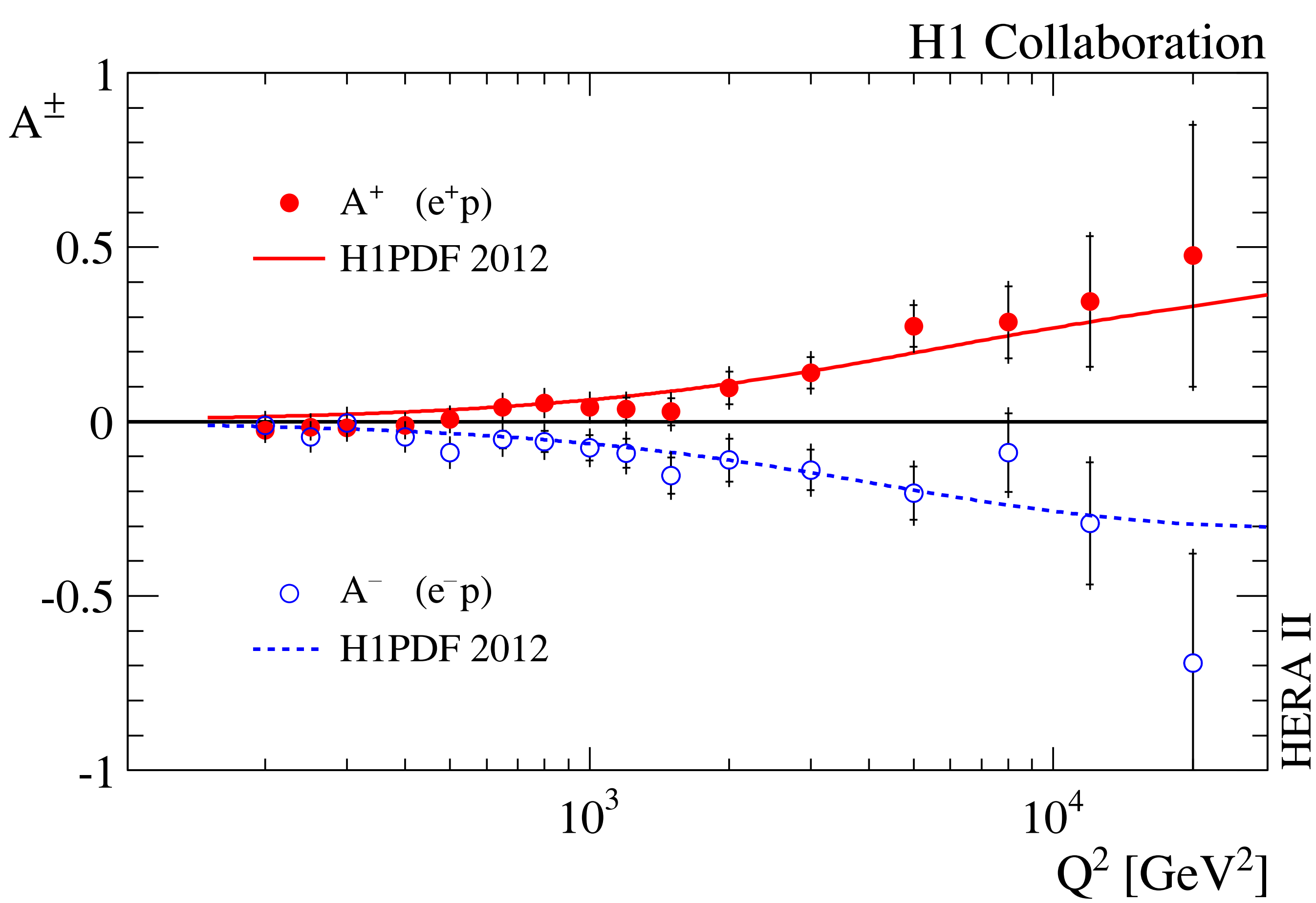

Measuring the difference in NC polarised cross sections gives access to new structure functions:

$$\frac{\sigma^{\pm}(P_L^{\pm}) - \sigma^{\pm}(P_R^{\pm})}{P_L^{\pm} - P_R^{\pm}} = \frac{\kappa Q^2}{Q^2 + M_Z^2}\left[\mp a_e F_2^{\gamma Z} + \frac{Y_-}{Y_+} v_e x F_3^{\gamma Z} - \frac{Y_-}{Y_+}\frac{\kappa Q^2}{Q^2 + M_Z^2}(v_e^2 + a_e^2) x F_3^Z\right]$$

xF_3 terms eliminated by subtracted e^-p from e^+p

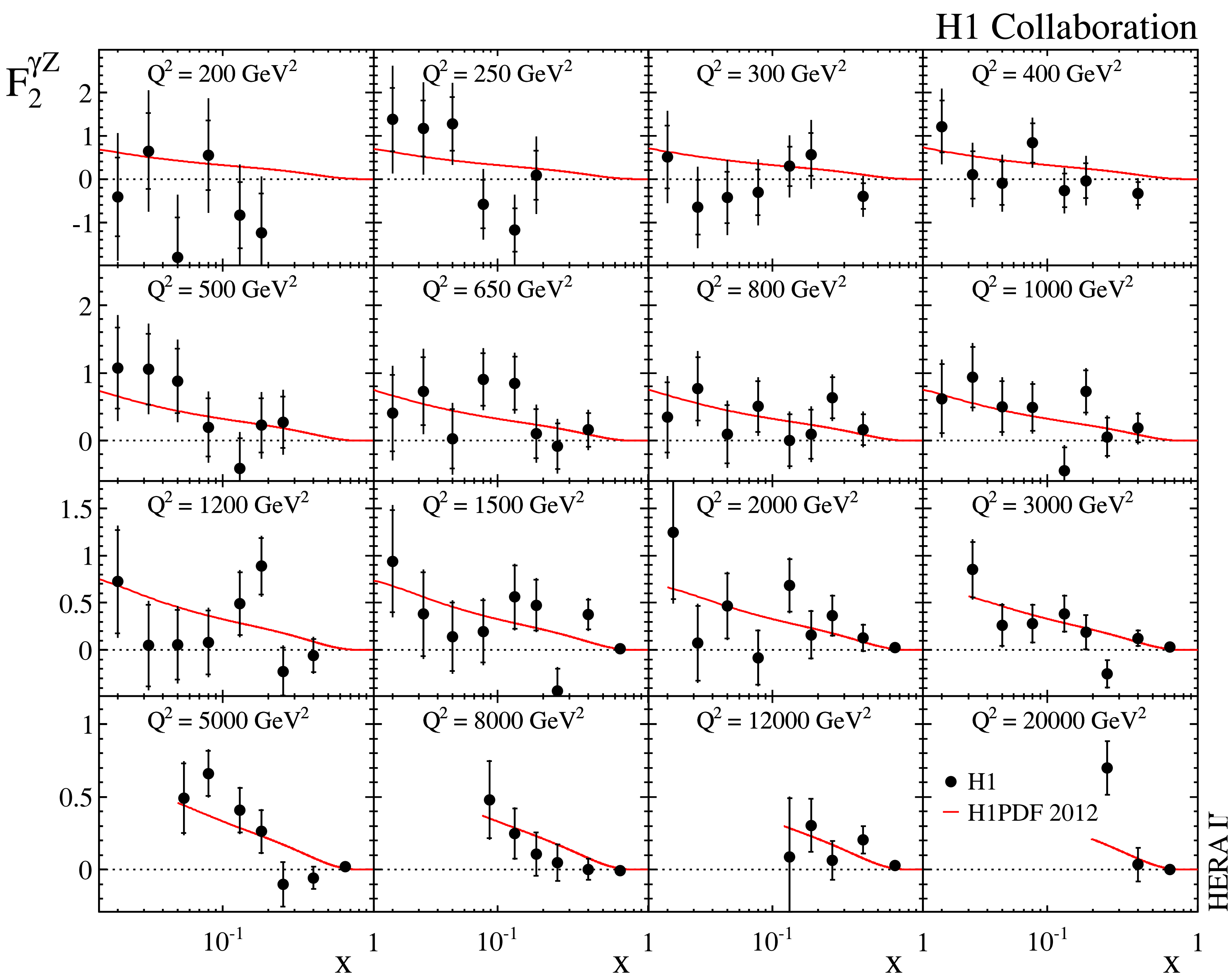

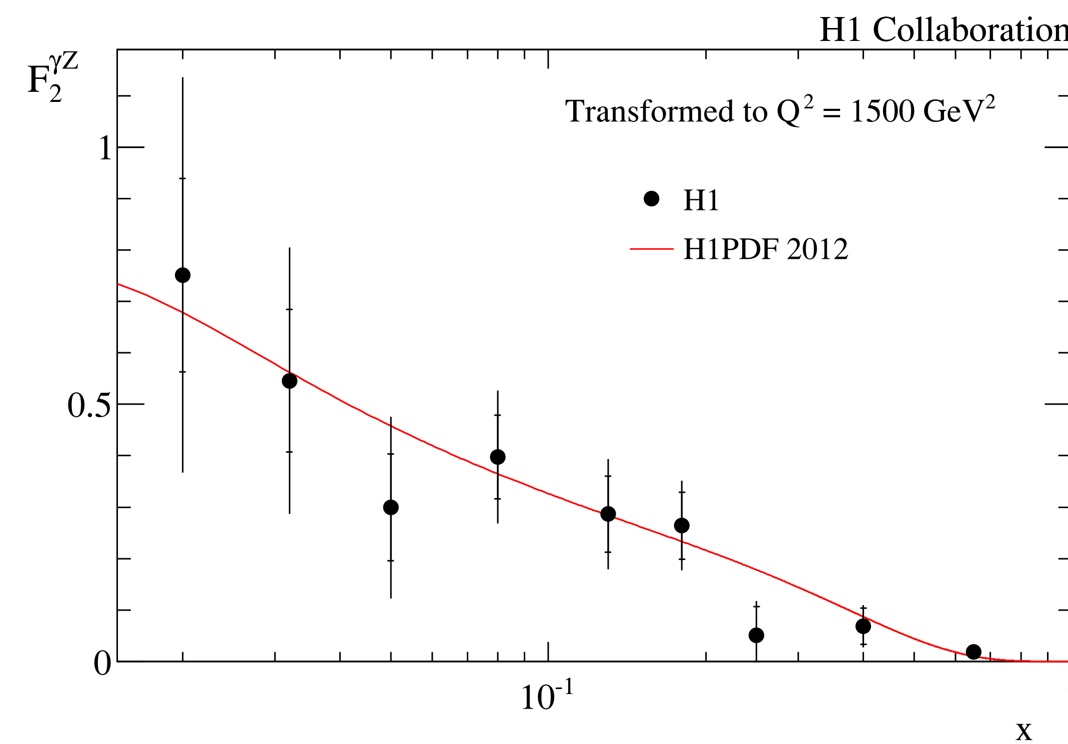

Combined H1 Data

New H1 data are combined with all previously published H1 inclusive cross section measurements

854 data points averaged to 413 measurements
χ^2/ndf = 412/441 = 0.93

Normalisation shifts for H1 data after averaging

Source	Shift in units of standard deviation	Shift in % of cross section
$\delta^{\mathcal{L}1}$ (BH Theory)	-0.39	-0.19
$\delta^{\mathcal{L}2}$ (e^+ 94-97)	-0.46	-0.66
$\delta^{\mathcal{L}3}$ (e^- 98-99)	-0.69	-1.20
$\delta^{\mathcal{L}4}$ (e^+ 99-00)	-0.07	-0.10
$\delta^{\mathcal{L}5}$ (QEDC)	0.81	1.70
$\delta^{\mathcal{L}6}, \delta^{\mathcal{L}7}$ (e^+L+R)	0.84	0.80
$\delta^{\mathcal{L}8}, \delta^{\mathcal{L}9}$ (e^-L+R)	0.84	0.89

Precision medium Q^2 HERA-I data ~unshifted

New high Q^2 HERA-II data shifted by ~1.7% (less than 1 std.dev)

New PDF fit performed: can be thought of as a 'stepping-stone' towards HERAPDF2.0

$$
\begin{aligned}
xg(x) &= A_g x^{B_g}(1-x)^{C_g} - A'_g x^{B'_g}(1-x)^{25}\,,\\
xu_v(x) &= A_{u_v} x^{B_{u_v}}(1-x)^{C_{u_v}}\left(1+E_{u_v}x^2\right)\,,\\
xd_v(x) &= A_{d_v} x^{B_{d_v}}(1-x)^{C_{d_v}}\,,\\
x\overline{U}(x) &= A_{\overline{U}} x^{B_{\overline{U}}}(1-x)^{C_{\overline{U}}}\,,\\
x\overline{D}(x) &= A_{\overline{D}} x^{B_{\overline{D}}}(1-x)^{C_{\overline{D}}}\,.
\end{aligned}
$$

Parameter	Central Value	Lower Limit	Upper Limit
f_s	0.31	0.23	0.38
m_c (GeV)	1.4	1.35 (for $Q^2_0 = 1.8$ GeV)	1.65
m_b (GeV)	4.75	4.3	5.0
$Q^2_{\rm min}$ (GeV^2)	3.5	2.5	5.0
Q^2_0 (GeV^2)	1.9	1.5 ($f_s = 0.29$)	2.5 ($m_c = 1.6$, $f_s = 0.34$)

13 parameter fit: additional flexibility given to u_v and d_v compared to H1PDF2009 / HERAPDF1.0

Apply momentum/counting sum rules:

$$\int_0^1 dx \cdot (xu_v + xd_v + x\bar{U} + x\bar{D} + xg) = 1$$

$$\int_0^1 dx \cdot u_v = 2 \qquad \int_0^1 dx \cdot d_v = 1$$

Parameter constraints:
$B_{\rm Ubar} = B_{\rm Dbar}$
sea = 2 x (Ubar +Dbar)
Ubar = Dbar at x=0
f_s = sbar/Dbar

Q_0^2 = 1.9 GeV^2 (below m_c)
Q^2 > 3.5 GeV^2
2 x 10^{-4} < x < 0.65
Fits performed using RT-VFNS

Experimental uncertainties produced using RMS spread of 400 replica fits
Parameterisation uncertainty determined from envelope of 14 parameter fit & Q_0^2 variations
Error band is applied to central value fit ⇒ asymmetric errors since mean of replicas ≠ central fit

$$\chi^2 = \sum_i \frac{\left[\mu_i - m_i\left(1-\sum_j \gamma^i_j b_j\right)\right]^2}{\delta^2_{i,{\rm unc}} m_i^2 + \delta^2_{i,{\rm stat}}\mu_i m_i\left(1-\sum_j \gamma^i_j b_j\right)} + \sum_j b_j^2 + \sum_i \ln\frac{\delta^2_{i,{\rm unc}} m_i^2 + \delta^2_{i,{\rm stat}}\mu_i m_i}{\delta^2_{i,{\rm unc}} \mu_i^2 + \delta^2_{i,{\rm stat}}\mu_i^2}$$

modified χ^2 definition includes ln term to account for likelihood transition to χ^2 after error scaling

H1PDF 2012

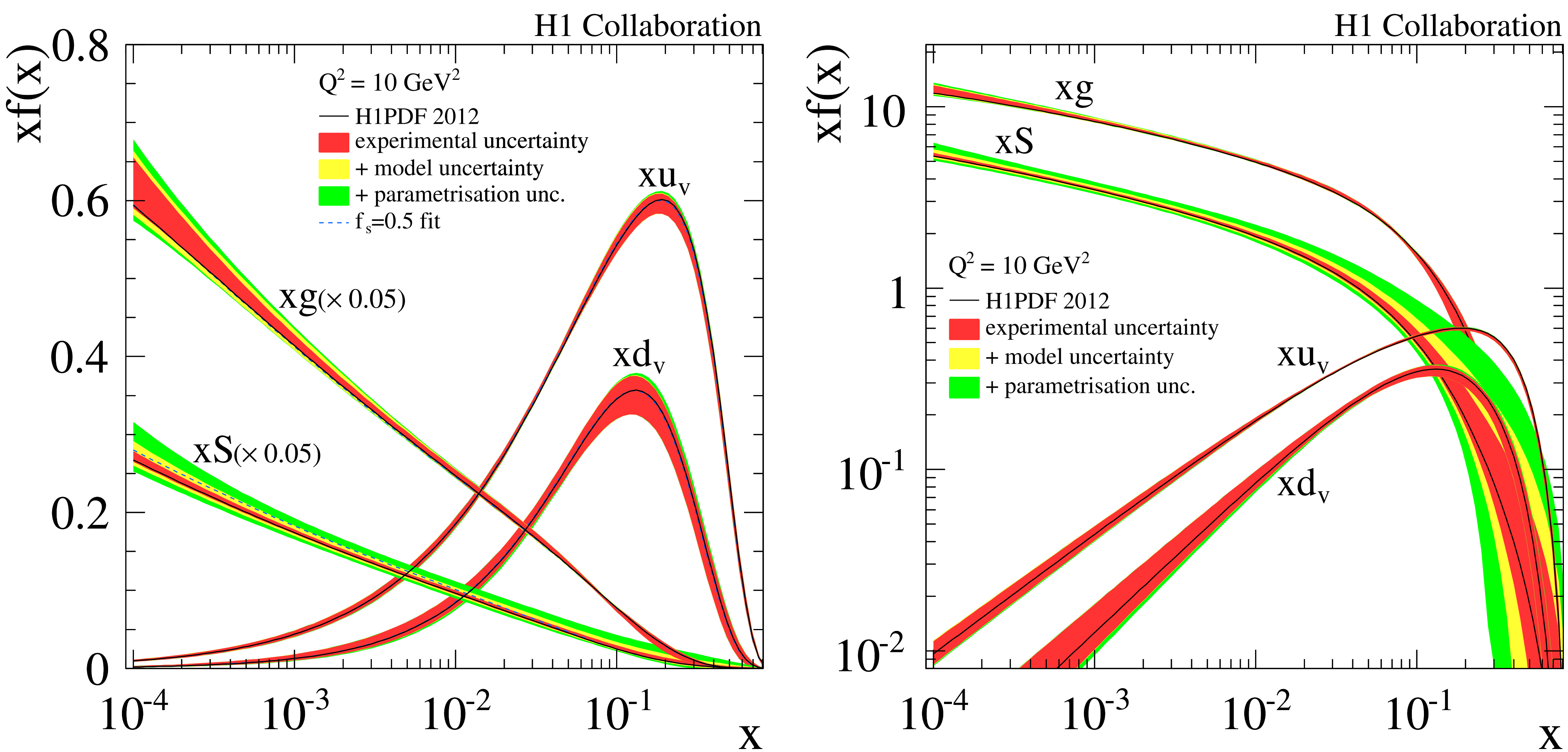

χ^2/ndf = 1570/1461 = 1.07

Fit with unsuppressed strange sea (f_s=0.5) is well within error bands

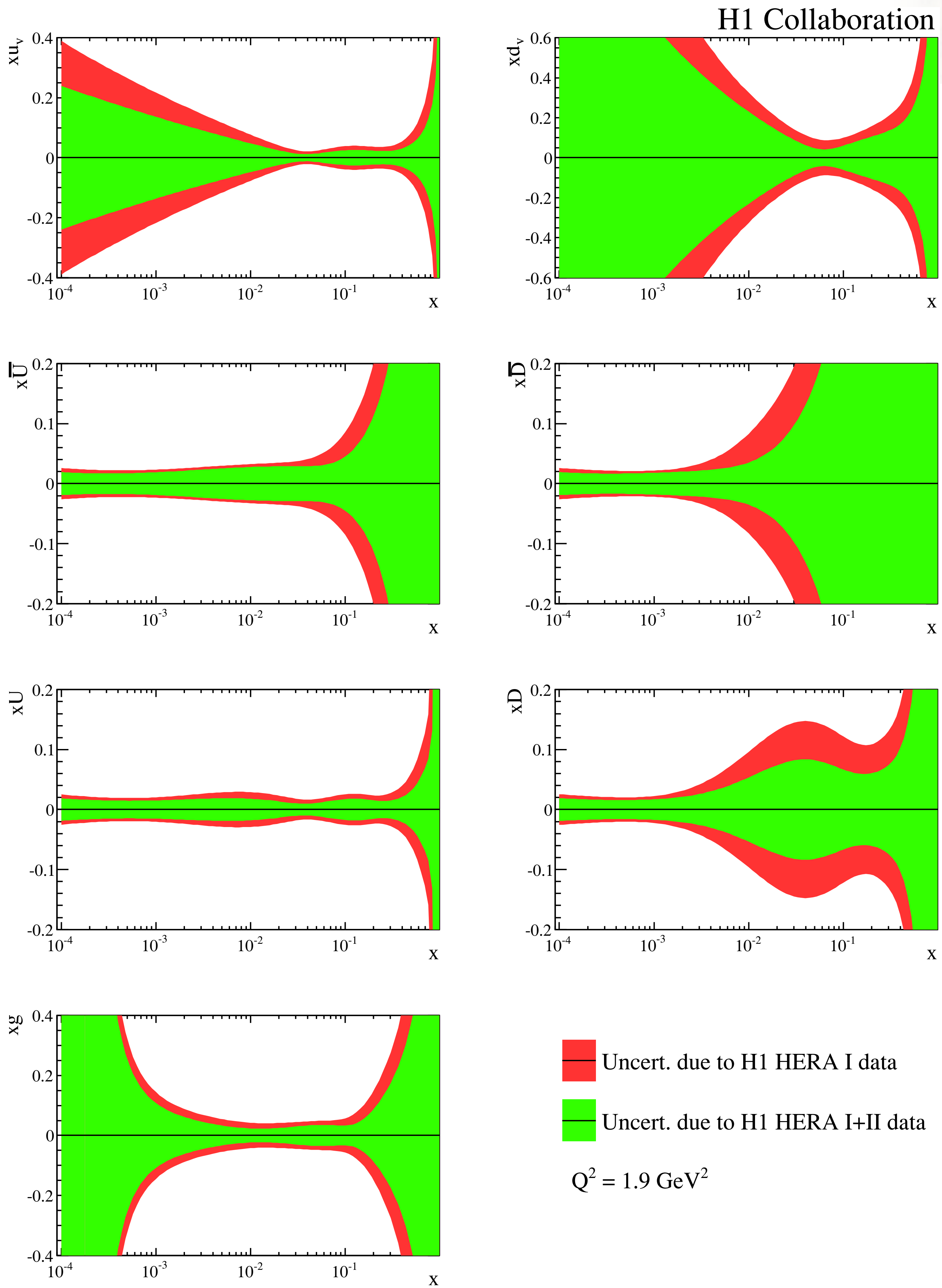

Comparison of PDF uncertainties from H1 fits with and without new HERA-II data

Large improvement in xd_v and xD over wide x range - driven by more precise CC e^+p data

Improvement in xu_v from NC at high x.
Error reduction at low x arises from sum rules

High x gluon is also improved from scaling violations

Compendium for HERAPDF

HERAPDF1.0
Combine NC and CC HERA-I data from H1 & ZEUS
Complete MSbar NLO fit
NLO: standard parameterisation with10 parameters
α_s = 0.1176 (fixed in fit)

HERAPDF1.5
Include additional NC and CC HERA-II data
Complete MSbar NLO and NNLO fit
NLO: standard parameterisation with 10 parameters

HERAPDF1.5f
NNLO: extended fit with 14 parameters

HERAPDF1.6
Include additional NC inclusive jet data $5 < Q^2 < 15000$
Complete MSbar NLO fit
NLO: standard parameterisation with 14 parameters
α_s = 0.1202 ± 0.0013 (exp) ± 0.004 (scales) free in fit

HERAPDF1.7
Include 41 additional F_2^{cc} data $4 < Q^2 < 1000$
Include 224 combined cross section points E_p=575/460 GeV
Complete MSbar NLO fit
NLO: standard parameterisation with 14 parameters

HERAPDF2.0
Include final:
HERA-I low/medium Q^2 precision F_2
HERA-II high Q^2 polarised NC/CC data
HERA-II low/medium energy NC data
HERA-I+II F_2^{cc} combined data - almost ready
HERA-I+II multijet data - awaiting H1 publication

Combined F_2^{cc} now at 2nd stage of internal review

Expect journal submission ~ early Nov.

Final structure function measurements from H1 / ZEUS now published
Combination of the data is underway
New combination will include:
- HERA-I published data
- HERA-II published data
- low/medium energy E_P=575/460 GeV run data

Expect several fits:
- NLO vs NNLO
- NLO will be: inclusive NC/CC data & inclusive + F_2^{cc} (+ jets?)
- Include fit to α_S
- MC method for experimental errors will be used

Timescale ~ spring 2013 (DIS workshop?)

Conclusions

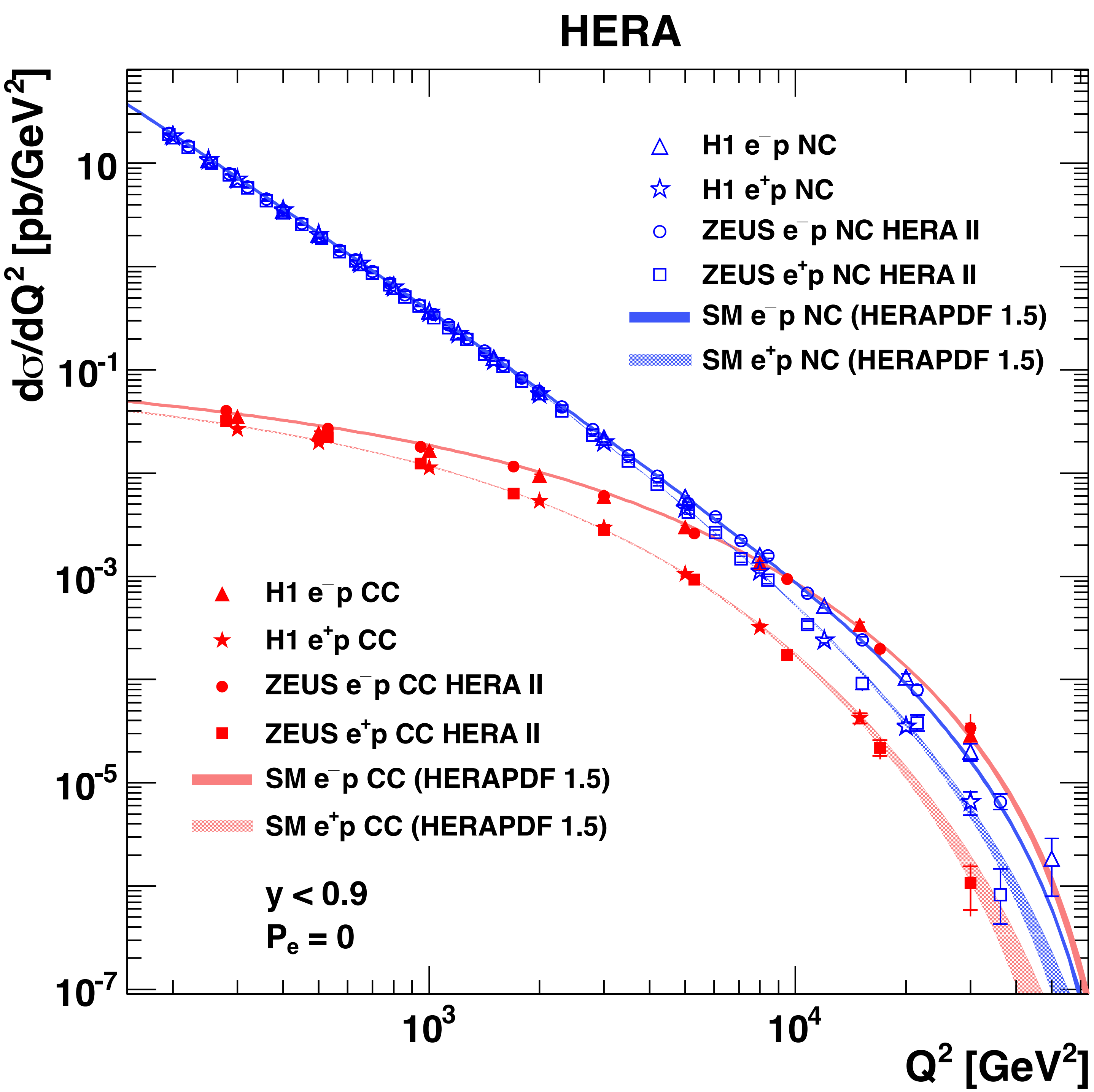

- H1 / ZEUS completed their final SF measurements
- New HERA-II data provide tighter constraints at high x / Q^2
- These data provide some of the most stringent constraints on PDFs
- Stress-test of QCD over 4 orders of mag. in Q^2
- DGLAP evolution works very well
- HERA data provide a self-consistent data set for complete flavour decomposition of the proton
- New combination of HERA data underway
- Combination ⇒ HERAPDF2.0 QCD fit

Backup Slides

H1 Systematic Error Source Correlation

Data set	$\delta^{\mathcal{L}}$		δ^{E}	δ^{θ}	δ^{h}	δ^{N}	δ^{B}	δ^{V}	δ^{S}	δ^{pol}
e^+ Combined low Q^2	$\delta^{\mathcal{L}1}$									
e^+ Combined low E_p	$\delta^{\mathcal{L}1}$									
e^+ NC 94-97	$\delta^{\mathcal{L}1}$	$\delta^{\mathcal{L}2}$	δ^{E1}	$\delta^{\theta 1}$	δ^{h1}	δ^{N1}	δ^{B1}	–	–	–
e^+ CC 94-97	$\delta^{\mathcal{L}1}$	$\delta^{\mathcal{L}2}$	–	–	δ^{h1}	δ^{N1}	δ^{B1}	δ^{V1}	–	–
e^- NC 98-99	$\delta^{\mathcal{L}1}$	$\delta^{\mathcal{L}3}$	δ^{E1}	$\delta^{\theta 2}$	δ^{h1}	δ^{N1}	δ^{B1}	–	–	–
e^- NC 98-99 *high* y	$\delta^{\mathcal{L}1}$	$\delta^{\mathcal{L}3}$	δ^{E1}	$\delta^{\theta 2}$	δ^{h1}	δ^{N1}	–	–	δ^{S1}	–
e^- CC 98-99	$\delta^{\mathcal{L}1}$	$\delta^{\mathcal{L}3}$	–	–	δ^{h1}	δ^{N1}	δ^{B1}	δ^{V2}	–	–
e^+ NC 99-00	$\delta^{\mathcal{L}1}$	$\delta^{\mathcal{L}4}$	δ^{E1}	$\delta^{\theta 2}$	δ^{h1}	δ^{N1}	δ^{B1}	–	δ^{S1}	–
e^+ CC 99-00	$\delta^{\mathcal{L}1}$	$\delta^{\mathcal{L}4}$	–	–	δ^{h1}	δ^{N1}	δ^{B1}	δ^{V2}	–	–
e^+ NC *high* y	$\delta^{\mathcal{L}5}$	$\delta^{\mathcal{L}6}, \delta^{\mathcal{L}7}$	δ^{E2}	$\delta^{\theta 3}$	δ^{h2}	δ^{N2}	–	–	δ^{S2}	–
e^- NC *high* y	$\delta^{\mathcal{L}5}$	$\delta^{\mathcal{L}8}, \delta^{\mathcal{L}9}$	δ^{E2}	$\delta^{\theta 3}$	δ^{h2}	δ^{N2}	–	–	δ^{S2}	–
e^+ NC L	$\delta^{\mathcal{L}5}$	$\delta^{\mathcal{L}6}$	δ^{E2}	$\delta^{\theta 3}$	δ^{h2}	δ^{N2}	δ^{B1}	–	–	δ^{P1}
e^+ CC L	$\delta^{\mathcal{L}5}$	$\delta^{\mathcal{L}6}$	–	–	δ^{h2}	δ^{N3}	δ^{B1}	δ^{V3}	–	δ^{P1}
e^+ NC R	$\delta^{\mathcal{L}5}$	$\delta^{\mathcal{L}7}$	δ^{E2}	$\delta^{\theta 3}$	δ^{h2}	δ^{N2}	δ^{B1}	–	–	δ^{P2}
e^+ CC R	$\delta^{\mathcal{L}5}$	$\delta^{\mathcal{L}7}$	–	–	δ^{h2}	δ^{N3}	δ^{B1}	δ^{V3}	–	δ^{P2}
e^- NC L	$\delta^{\mathcal{L}5}$	$\delta^{\mathcal{L}8}$	δ^{E2}	$\delta^{\theta 3}$	δ^{h2}	δ^{N2}	δ^{B1}	–	–	δ^{P3}
e^- CC L	$\delta^{\mathcal{L}5}$	$\delta^{\mathcal{L}8}$	–	–	δ^{h2}	δ^{N3}	δ^{B1}	δ^{V3}	–	δ^{P3}
e^- NC R	$\delta^{\mathcal{L}5}$	$\delta^{\mathcal{L}9}$	δ^{E2}	$\delta^{\theta 3}$	δ^{h2}	δ^{N2}	δ^{B1}	–	–	δ^{P4}
e^- CC R	$\delta^{\mathcal{L}5}$	$\delta^{\mathcal{L}9}$	–	–	δ^{h2}	δ^{N3}	δ^{B1}	δ^{V3}	–	δ^{P4}

correlation of H1 systematic error sources

$\delta^{\mathcal{L}1}$ → 0.5% BH theoretical error HERA-I

$\delta^{\mathcal{L}5}$ → 2.3% Compton lumi error HERA-II

$\delta^{\mathcal{L}\text{6-9}}$ → 1.5% Compton unc. error HERA-II

Data Period	Global Normalisation	Per Period Normalisation	Total Normalisation
e^+ Combined low Q^2	0.993	–	0.993
e^+ Combined low E_p	0.993	–	0.993
HERA I e^+ 94-97	0.993	0.999	0.992
HERA I e^- 98-99	0.993	1.003	0.996
HERA I e^+ 99-00	0.993	1.005	0.998
HERA II e^+ L	1.029	0.991	1.020
HERA II e^+ R	1.029	1.013	1.042
HERA II e^- L	1.029	1.010	1.039
HERA II e^- R	1.029	1.014	1.043

normalisations from H1PDF 2012

Low Q^2 data shifted by -0.7%
HERA-1 high Q^2 by -0.3%
HERA-II high Q^2 by +2 to +4%

All shifts are <1.3 std.devs

<u>HERAPDF1.0</u>
Combine NC and CC HERA-I data from H1 & ZEUS
Complete MSbar NLO fit
NLO: standard parameterisation with10 parameters
$\alpha_s = 0.1176$ (fixed in fit)

desy-09-158

<u>HERAPDF1.5</u>
Include additional NC and CC HERA-II data
Complete MSbar NLO and NNLO fit
NLO: standard parameterisation with10 parameters
<u>HERAPDF1.5f</u>
NNLO: extended fit with 14 parameters

H1-10-142 / ZEUS-prel-10-018

$$xf(x,Q_0^2) = A \cdot x^B \cdot (1-x)^C \cdot (1 + Dx + Ex^2)$$

$$xg,\quad xu_v,\quad xd_v,\quad x\bar{U},\quad x\bar{D} \longrightarrow xg,\quad xU = xu + xc,\quad xD = xd + xs,\quad x\bar{U} = x\bar{u} + x\bar{c},\quad x\bar{D} = x\bar{d} + x\bar{s} \longrightarrow$$

$$\begin{aligned}
xg(x) &= A_g x^{B_g}(1-x)^{C_g}, \\
xu_v(x) &= A_{u_v} x^{B_{u_v}}(1-x)^{C_{u_v}}\left(1 + E_{u_v}x^2\right), \\
xd_v(x) &= A_{d_v} x^{B_{d_v}}(1-x)^{C_{d_v}}, \\
x\bar{U}(x) &= A_{\bar{U}} x^{B_{\bar{U}}}(1-x)^{C_{\bar{U}}}, \\
x\bar{D}(x) &= A_{\bar{D}} x^{B_{\bar{D}}}(1-x)^{C_{\bar{D}}}.
\end{aligned}$$

$x\bar{s} = f_s x\bar{D}$ strange sea is a fixed fraction f_s of $\bar{D}$ at Q_0^2

Apply momentum/counting sum rules:

$$\int_0^1 dx \cdot (xu_v + xd_v + x\bar{U} + x\bar{D} + xg) = 1$$

$$\int_0^1 dx \cdot u_v = 2 \qquad \int_0^1 dx \cdot d_v = 1$$

Parameter constraints:
$B_{uv} = B_{dv}$
$B_{Ubar} = B_{Dbar}$
sea = 2 x (Ubar +Dbar)
Ubar = Dbar at x=0

Q_0^2 = 1.9 GeV^2 (below m_c)
Q^2 > 3.5 GeV^2
$2 \times 10^{-4} < x < 0.65$
Fits performed using RT-VFNS

HERAPDF1.0 central values:

	A	B	C	E
xg	6.8	0.22	9.0	
xu_v	3.7	0.67	4.7	9.7
xd_v	2.2	0.67	4.3	
$x\bar{U}$	0.113	−0.165	2.6	
$x\bar{D}$	0.163	−0.165	2.4	

χ^2/ndf = 574/582

Experimental systematic sources of uncertainty allowed to float in fit
Include model assumptions into uncertainty:
f_s , m_c , m_b , Q^2_0, Q^2_{min}

Variation	Standard Value	Lower Limit	Upper Limit
f_s	0.31	0.23	0.38
m_c [GeV]	1.4	$1.35^{(a)}$	1.65
m_b [GeV]	4.75	4.3	5.0
Q^2_{min} [GeV^2]	3.5	2.5	5.0
Q^2_0 [GeV^2]	1.9	$1.5^{(b)}$	$2.5^{(c,d)}$

$^{(a)}Q_0^2 = 1.8$ $^{(c)}m_c = 1.6$
$^{(b)}f_s = 0.29$ $^{(d)}f_s = 0.34$

Excellent consistency of input data allow standard statistical error definition:
$\Delta\chi^2 = 1$

Exclusive jet data required for free α_s fit
See talk of Krzysztof Nowak

In 14 parameter fit:
release $B_{uv} = B_{dv}$ constraint
allow more flexible gluon

$$xg(x,Q_0^2) = A \cdot x^B \cdot (1-x)^C - A' \cdot x^{B'} \cdot (1-x)^{25}$$

allows for valence-like or negative gluon at Q_0^2

Charm Content of the Proton

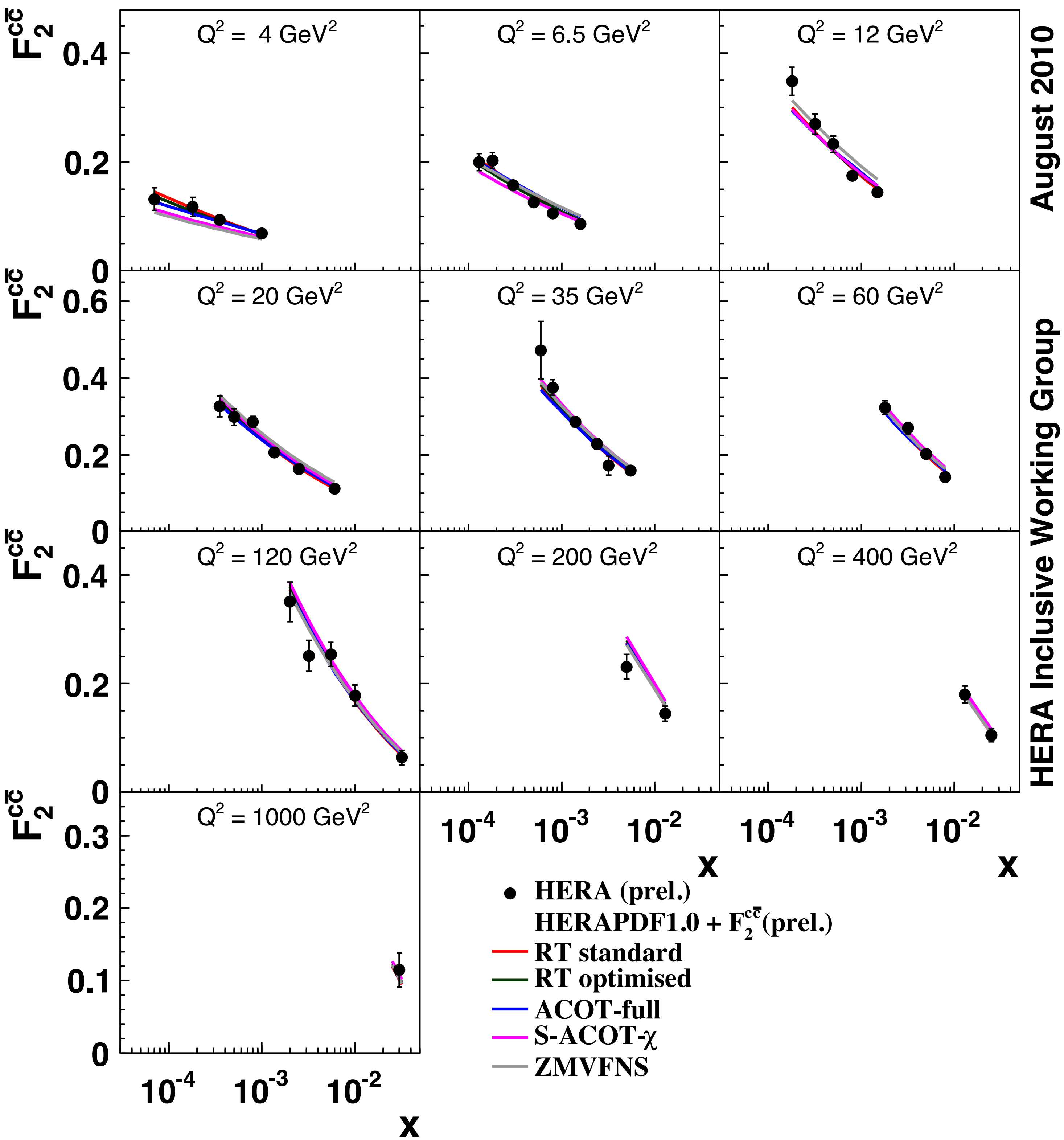

The inclusive charm content of proton can be measured in several methods: D* decays , impact parameter significance... Combination yields ~5-10% precision

Data cover wide phase space region including charm threshold region

Theory predictions have small spread
⇒ use optimised m_c parameter

Spread of LHC Z/W production predictions is reduced ~4.5% → ~0.7%
when using optimal value of m_c

DIS Jet Cross Sections

ZEUS inclusive jets	39 pb^{-1}	$Q^2 > 125$	Nucl. Phys. B765 (2007) 1-30
ZEUS inclusive jets	82 pb^{-1}	$Q^2 > 125$	Phys. Lett. B649 (2007) 12
H1 inclusive jets	395 pb^{-1}	$150 < Q^2 < 15000$	EPJ C65 (2010) 363-383
H1 inclusive jets	44 pb^{-1}	$5 < Q^2 < 100$	EPJ C67 (2010) 1-24

Jet data bring significant sensitivity to α_S
Disentangles correlation between $xg(x,Q^2)$ and α_S

HERAPDF1.6 : Simultaneous NLO QCD fit to
- combined NC inclusive cross section data
- combined CC inclusive cross sections data
- normalised H1/ZEUS inclusive jet data

$$\alpha_S(M_Z) = 0.1202 \pm 0.0013 \text{ (exp)} \\ \pm 0.0007 \text{ (model)} \\ \pm 0.0012 \text{ (hadronisation)} \\ {}^{+0.0045}_{-0.0036} \text{ (scales)}$$

Only combined PDF / α_S fit on the market

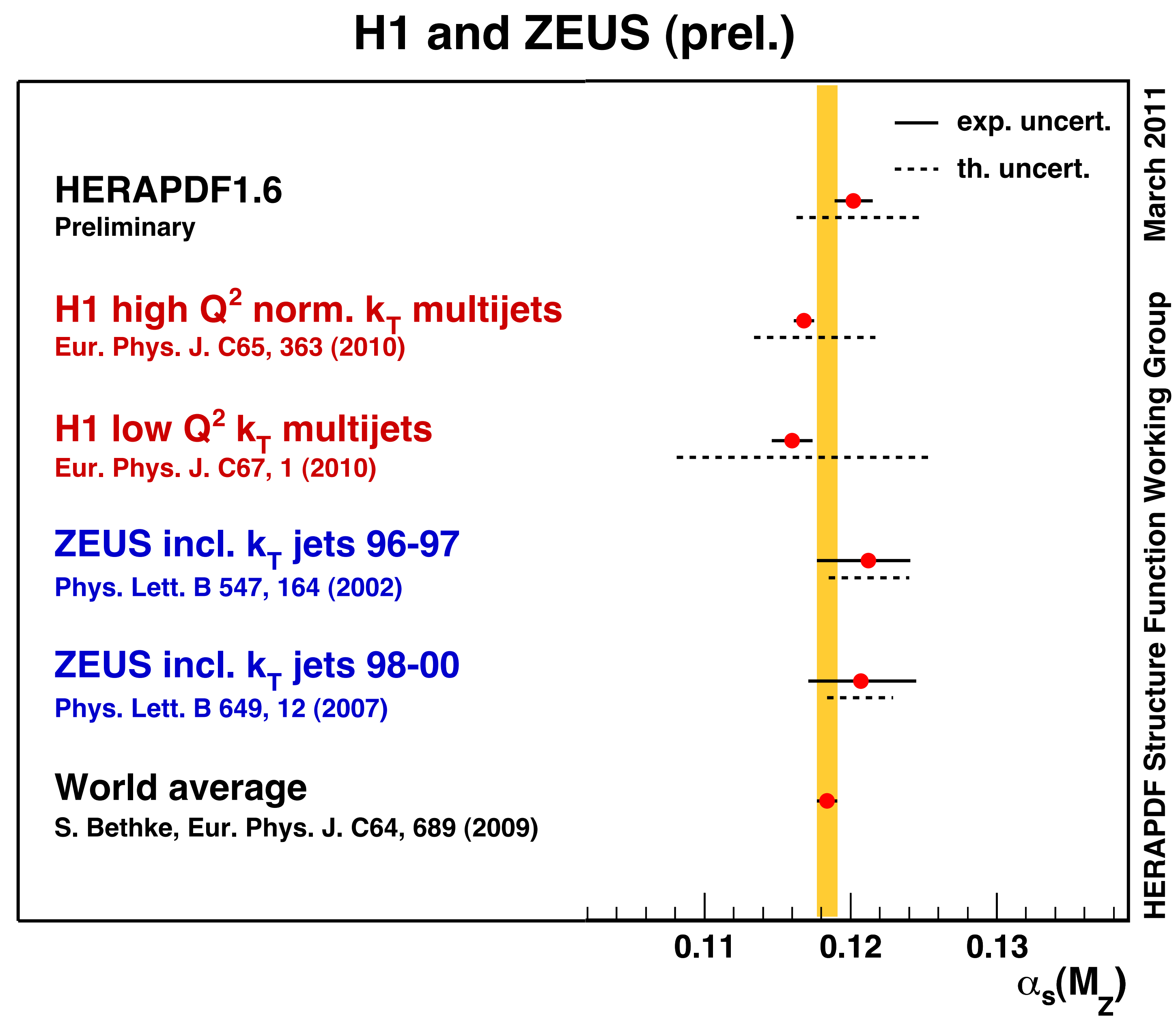

High Q^2 NC Multi-jets

H1prelim-11-032

New H1 measurement of inclusive, dijet and trijet rates

<u>First measurement</u> of double diff'l trijet cross section

Significantly reduced systematic errors

1% hadronic scale uncertainty

For now - unnormalised cross sections...

Jets in Breit frame: $5 < P_T < 50$ GeV
$M_{12} > 16$ GeV

Greater sensitivity to α_s with more jets

High Q^2 and large jet $P_T \Rightarrow$ multi-scale QCD problem

Good description in NLO

(worse for di-jets at low $\langle P_T \rangle$ ...)

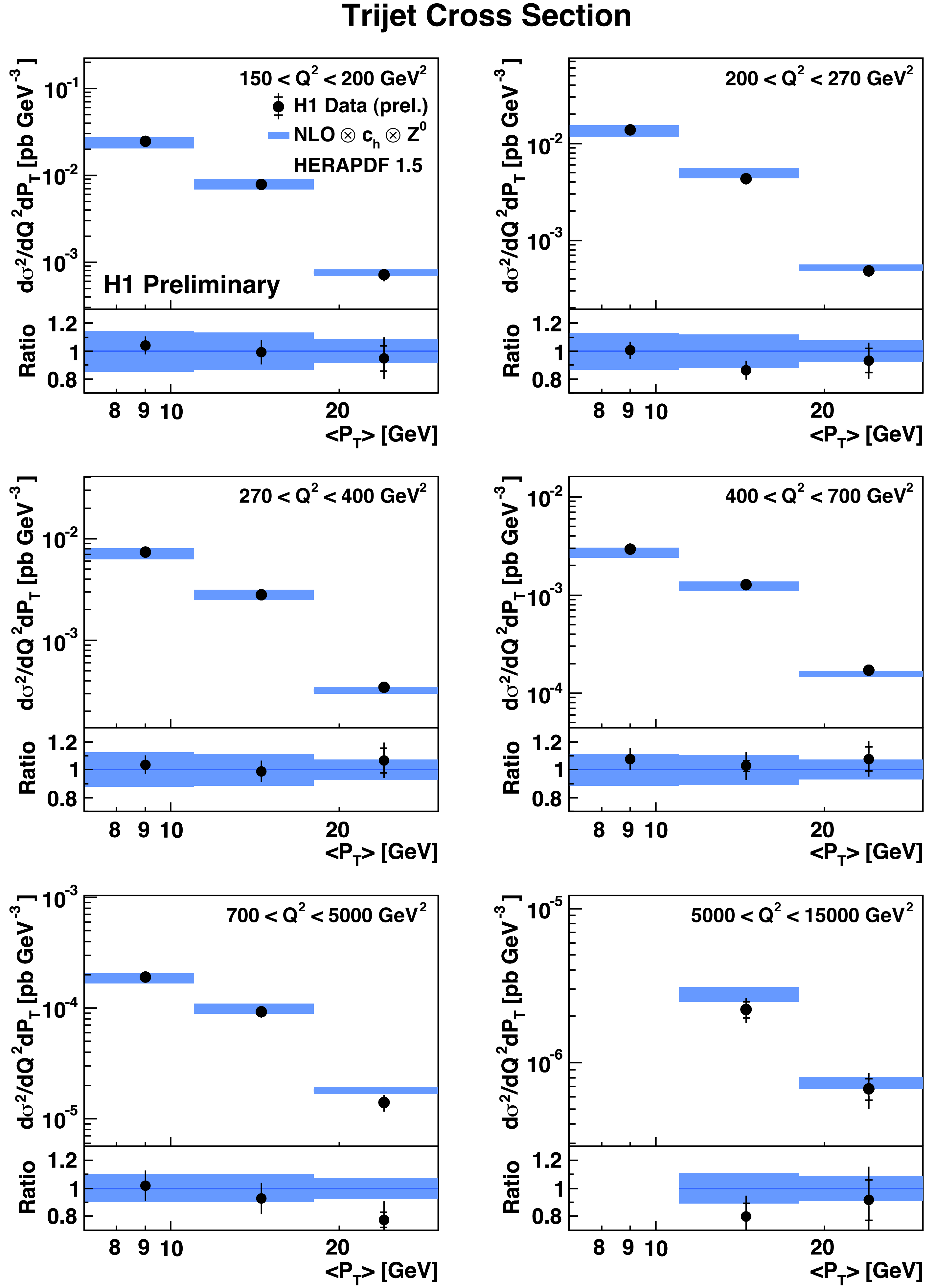

NLO calculation $\mu_R = \mu_F = \sqrt{\frac{1}{2}(Q^2 + P_T^2)}$

scales varied by factors of 2 for uncertainty

High Q^2 NC Multi-jets

H1prelim-11-032

Di-jet rates in reasonable agreement

~10% discrepancy at low $\langle P_T \rangle$

Data want smaller α_s or smaller xg ?

Extract α_s independently for each jet data set in NLO

PDF uncertainty from CT10 error propagation

Inclusive jets:

$$\alpha_s(M_Z) = 0.1190 \pm 0.0021(exp.) \pm 0.0020(pdf)^{+0.0050}_{-0.0056}(th.)$$

Dijets:

$$\alpha_s(M_Z) = 0.1146 \pm 0.0022(exp.) \pm 0.0021(pdf)^{+0.0044}_{-0.0045}(th.)$$

Trijets:

$$\alpha_s(M_Z) = 0.1196 \pm 0.0016(exp.) \pm 0.0010(pdf)^{+0.0055}_{-0.0039}(th.)$$

Achieved ~1% experimental precision on α_s

Theoretical uncertainty (scales) dominate ~4%

PDF uncertainty ~1%

To come:

Use of normalised cross sections

cancellation of systematic uncertainties

→ reduced error for α_s

Dijet Cross Section